Journal of Medicinal Chemistry

Article

pubs.acs.org/jmc

Kinase Scaffold Repurposing for Neglected Disease Drug Discovery: Discovery of an Efficacious, Lapatanib-Derived Lead Compound for Trypanosomiasis

Gautam Patel,[†] Caitlin E. Karver,[†] Ranjan Behera,[‡] Paul J. Guyett,[‡] Catherine Sullenberger,[‡] Peter Edwards,[†] Norma E. Roncal,[§] Kojo Mensa-Wilmot,*[,‡] and Michael P. Pollastri*[,†]

[†]Department of Chemistry and Chemical Biology and Center for Drug Discovery, Northeastern University, Boston, Massachusetts 02115, United States

[‡]Department of Cellular Biology, University of Georgia, Athens, Georgia 30602, United States

[§]Walter Reed Army Institute of Research, Silver Spring, Maryland 20910, United States

Supporting Information

ABSTRACT: Human African trypanosomiasis (HAT) is a neglected tropical disease caused by the protozoan parasite *Trypanosoma brucei*. Because drugs in use against HAT are toxic and require intravenous dosing, new drugs are needed. Initiating lead discovery campaigns by using chemical scaffolds from drugs approved for other indications can speed up drug discovery for neglected diseases. We demonstrated recently that the 4-anilinoquinazolines lapatinib (GW572016, **1**) and canertinib (CI-1033) kill *T. brucei* with low micromolar EC_{50} values. We now report promising activity of analogues of **1**, which provided an excellent starting point for optimization of the chemotype. Our compound optimization that has led to synthesis of several potent 4-anilinoquinazolines, including NEU617, **23a**, a highly potent, orally bioavailable inhibitor of trypanosome replication. At the cellular level, **23a** blocks duplication of the kinetoplast and arrests cytokinesis, making it a new chemical tool for studying regulation of the trypanosome cell cycle.

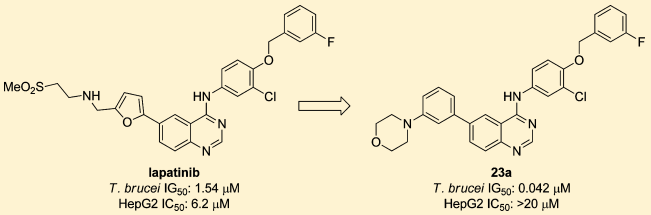

INTRODUCTION

Neglected tropical diseases (NTDs) represent a significant global health burden, particularly in developing regions of the world. Estimates of as many as one in six in the world population (over 1 billion people) are infected by one or more NTDs, with one in three people at risk.[1] These diseases are "neglected" because so few research dollars are invested in treating or preventing them, in comparison to those conditions primarily affecting the developed world. As a result, pragmatic and cost-effective approaches for identification of drug leads are needed in order to spawn the discovery of new drugs.

One such approach is to "repurpose" classes of proven molecular targets with essential homologues in the pathogens that cause these NTDs.[2] For example, *Trypanosoma brucei* (which causes human African trypanosomiasis (HAT), *Trypanosoma cruzi* (Chagas' disease), *Leishmania* spp. (causative agents for leishmaniases), and *Plasmodium* spp. (malaria) all express kinases and phosphodiesterases (PDEs) that are involved in aspects of cellular signaling.[3,4] Indeed, kinases and PDEs represent proven drug target classes in humans for a variety of indications and, as such, a large amount of data related to medicinal chemistry, toxicology, and structural biology are available that can potentially inform new optimization programs against parasites. Furthermore, the clinical and preclinical chemical matter itself can sometimes represent a starting point for new antiparasitic approaches, an approach demonstrated by us[5−7] and by others.[8,9]

Following parasite transmission via an infected tsetse fly, a trypanosome bloodstream infection gives rise to flu-like symptoms that eventually subside. At this point, the parasites invade the central nervous system (CNS), where they establish an infection that leads to sleep disruption, coma, and eventually death. Current drugs have less than optimal toxicity profiles, and the dosing regimens can be inconvenient, long, and costly. There is therefore a stated need for new HAT therapeutics that are orally administered, with minimal toxicity, and which are effective against both bloodstream and CNS forms of the disease. To that end, "hit" and "lead" criteria for HAT and other NTDs are clearly described.[10]

Kinase inhibitors have come to the fore as one of the principal enzyme target classes in drug discovery for a wide variety of indications, including cancer,[11] inflammation,[12,13] diabetes,[14,15] and CNS diseases.[16] In particular, a number of tyrosine kinase inhibitors have been approved for clinical use.[17] This list includes lapatinib (GW572016, Tykerb, **1**), an EGFR inhibitor that gained FDA approval in 2007.[18]

T. brucei expresses over 180 protein kinases,[19,20] some of which (such as glycogen synthase kinase-3,[21] phosphoinositol-

Received: November 27, 2012

   dx.doi.org/10.1021/jm400349k | *J. Med. Chem.* XXXX, XXX, XXX−XXX

Table 1. Initial Screening Data of Analogues of Lapatinib 1

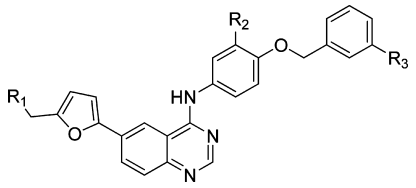

Compd	GSK Number	R_1	R_2	R_3	Tbb EC_{50} (μM)[a,b]
2	GW58337A	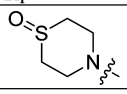	Cl	H	0.41
3	GW601906A	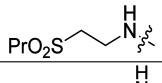	Cl	F	0.43
4	GW633460A	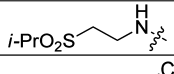	Cl	F	0.48
5	GW616030X	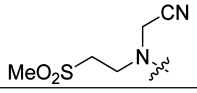	Cl	F	0.52
6	GW615311X	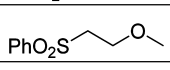	Cl	F	0.55
7	GW580496A	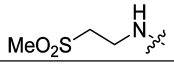	Br	H	0.56
8	GW576924A	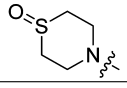	F	F	0.60
9	GW616907X	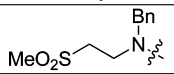	Cl	F	1.51
1	lapatinib	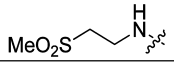	Cl	F	1.54
	melarsoprol[49]				0.0063
	eflornithine[50]				16.4
	pentamidine[49]				0.0035
	SCYX-7158[51]				0.794

[a]All EC_{50} values are ±7%. [b]Concentration giving 50% inhibition of growth of *T brucei brucei* Lister 427 cells.[49]

3-kinases/TOR,[7] and Aurora kinase 1[6]) have been targeted in drug discovery efforts already. There is unequivocal chemical data for protein Tyr phosphorylation in the parasite.[22,23] However, trypanosomes do not express receptor tyrosine kinases (RTKs),[4] and it is widely held that Tyr-phosphorylation must therefore be performed by dual-specificity enzymes (e.g., wee1) that act on Ser/Thr as well as Tyr residues.[4] Intriguingly, on the basis of bioinformatics analysis, enzymes with "EGFR-like" kinase domains are present in the parasite.[24] Further, inhibitors of human EGFR/HER2 (i.e., canertinib,[25] **1**,[26] and AEE788[27]) kill *T. brucei* with EC_{50} in the low micromolar range.[24]

Transferrin is a growth factor that *T. brucei* acquires from its vertebrate host by receptor-mediated endocytosis.[28] We discovered that receptor-mediated endocytosis of Tf in the African trypanosome is stimulated by diacylglycerol (DAG).[29] In most eukaryotes, effects of DAG on signaling pathways are amplified by the Ser/Thr kinase protein kinase C, which binds to the lipid with its C1-domain. In trypanosomes, DAG signaling pathways have not been studied. To understand the pathway linking DAG and Tf endocytosis in the trypanosome, we tested the effect of inhibitors of Ser/Thr protein kinases (e.g., protein kinase C) or Tyr kinases on DAG-stimulated endocytosis of Tf. Unexpectedly, DAG-stimulated endocytosis of Tf was not blocked by a Ser/Thr protein kinase inhibitor, nor does the genome of *T. brucei* encode for a classic PKC. Instead, the pathway was inhibited by a Tyr kinase inhibitor Tyrphostin A47, a tyrosine mimic.[30] In a related study, we found that **1**, similar to Tyrphostin A47, inhibited endocytosis of transferrin.[31]

These data suggested to us that tyrosine kinase inhibitor drugs approved for treatment of nonparasite human diseases were worth testing as antitrypanosomal agents. We have evaluated the trypanocidal properties of a panel of EGFR inhibitors provided by GlaxoSmithKline (Table 1), and we describe the subsequent design and synthesis of novel analogues for a structure−activity relationship study of a 6-phenyl 4-anilinoquinazoline scaffold, culminating in **23a**, a highly selective and potent inhibitor of trypanosome replication in vitro.

RESULTS

We obtained nine quinazoline-based EGFR inhibitors (**1**−**9**, Table 1)[18,32−34] from GlaxoSmithKline and screened them against cultures of *T brucei brucei* Lister 427. The inhibitors demonstrated a 4-fold range in potency (Table 1) within the limited scope in variation of the R^1 "tail" region of the scaffold. We noted the EC_{50} of **1** (1.54 μM) to be 4-fold more potent against *T. brucei* as compared to a HepG2 hepatocarcinoma cell line.[35] For comparison, we have also included in Table 1 the published activities of three front-line HAT treatments

dx.doi.org/10.1021/jm400349k | J. Med. Chem. XXXX, XXX, XXX−XXX

Scheme 1. Synthesis of Analogues 10[a]

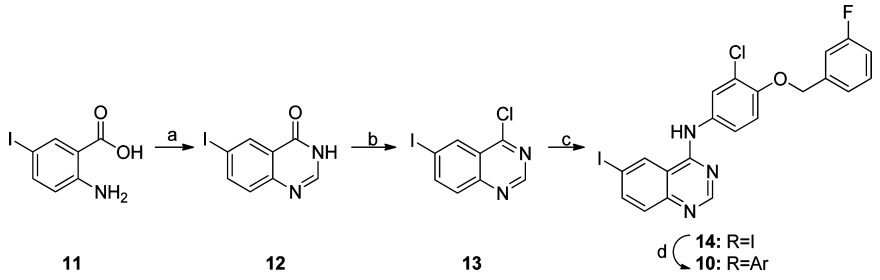

[a]Reagents and conditions: (a) formamide, 170 °C, 4 h, 70%; (b) thionyl chloride, DMF, 80 °C, 12 h, 85%; (c) 3-chloro-4-((3-fluorobenzyl)oxy)aniline, 2-propanol, 80 °C, 12 h, 85%; (d) Ar-B(OH)$_2$, Pd(PPh$_3$)$_4$, 2 M Na$_2$CO$_3$, DME, EtOH, 80 °C, 12 h.

(eflornithine, melarsoprol, and pentamidine) and of SCYX-7158, currently in clinical trials.[51] The goal of our subsequent optimization efforts have dwelt on improvement of the potency of this chemotype for inhibition of *T. brucei* replication and increasing the selectivity ratio over HepG2 cells.

Noting the effect of subtle tail-group changes on parasite growth inhibition, we first focused our attention on broader exploration of replacements for the furan-derived tail. This was achieved by a broad diversity scan utilizing Suzuki chemistry methodology using boronic acids or esters to enumerate a virtual library of analogues of **1** (Scheme 1). The structures in this 197-membered virtual library were clustered based on a maximum dissimilarity algorithm, and cluster centers were selected for synthesis (PipelinePilot, Scitegic, Inc.).

In anticipation of the parallel synthesis, we prepared the iodoquinazoline **14** by the route shown in Scheme 1. Treatment of the commercially available anthranilic acid **11** with formamide proceeded in 70% yield, followed by chlorination with thionyl chloride to provide the chloroquinazoline **13** in 85% yield. This template was reacted with the requisite aniline (**17**, Scheme 2), which was prepared by a sequence of alkylation of the nitrophenol **15** with 3-fluorobenzyl bromide followed by nitro group reduction.[50] With the required template **14** in hand, we prepared 10 analogues (**10a–j**) from the selected boronates using standard Suzuki reaction conditions. The structures and biological activities for these compounds are summarized in Table 2. From this series of analogues, we identified NEU369 (**10a**), which was approximately equipotent to **1** against *T brucei* cells. Further testing of this compound and its analogues showed that, unlike **1**, it did not inhibit HepG2 cell growth (EC_{50} > 15 μM) (Table 3).

Scheme 2. Synthesis of Requisite Aniline Intermediates 17[a]

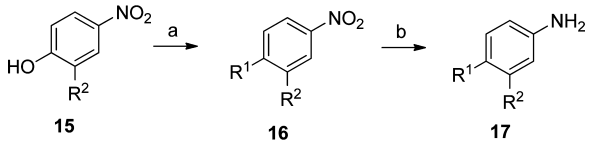

[a]Reagents and conditions: (a) alkyl halide, K_2CO_3, acetonitrile, 50 °C, 12 h; (b) Zn, NH_4Cl, MeOH, H_2O, 25–50 °C, 6 h.

Keeping the newly identified tail group present in **10a** (Table 3), we turned our attention to exploration of the aniline headgroup region of the molecule. Preparation of the requisite chloroquinazoline **19** (Scheme 3) was achieved by treatment of **12** with the required boronic acid using Suzuki conditions, followed by chlorination with thionyl chloride. This intermediate was reacted with a range of anilines (Scheme 2) to provide analogues **20** (Table 3).

Table 2. *T. brucei* Growth Inhibition Data of Diverse Analogues 10a–10j

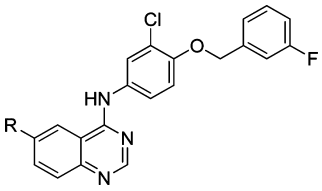

Compd	R	Tbb EC_{50} (μM)[a,b]
10a	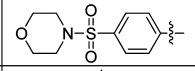	1.39
10b	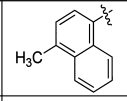	2.27
10c	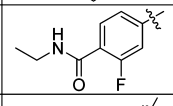	3.85
10d	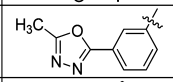	4.21
10e	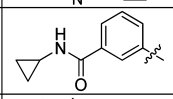	4.50
10f	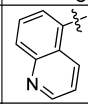	4.53
10g	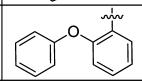	5.3
10h	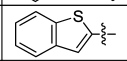	5.98
10i	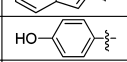	6.45
10j	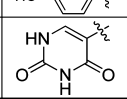	22.63

[a]All EC_{50} values are ±7%. [b]Concentration giving 50% inhibition of growth of *T brucei brucei* Lister 427 cells

This library was designed to explore the role of halogen substitutions on the terminal benzyl substituent (R^1) headgroup, testing positional isomers of fluoro substitutions and other potential halogen replacements such as methoxy and trifluoromethyl groups. These modifications produced insignificant changes in activity of the compounds against *T. brucei*. We prepared a few analogues to assess functional group tolerance at

dx.doi.org/10.1021/jm400349k | J. Med. Chem. XXXX, XXX, XXX–XXX

Table 3. *T. brucei* Growth Inhibition Data for Headgroup Variations of 10a

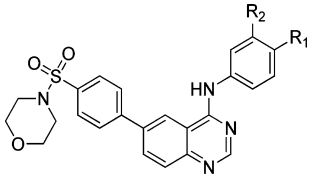

Compd	R_1	R_2	Tbb EC_{50} (μM)[a,b]	HepG2 IC_{50} (μM)
10a	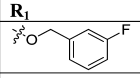	Cl	1.39	>15
20a	H	H	1.44	> 3
20b	CH_3	H	1.15	> 15
20c	OH	Cl	1.06	> 15
20d	OCH_3	Cl	0.82	> 15
20e	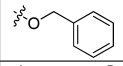	Cl	1.35	> 15
20f	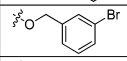	Cl	0.68	> 15
20g	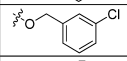	Cl	0.66	> 15
20h	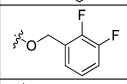	Cl	0.82	>15
20i	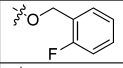	Cl	1.65	> 15
20j	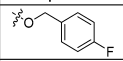	Cl	1.34	> 15
20k	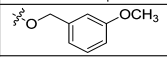	Cl	1.43	> 15
20l	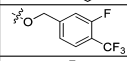	Cl	0.54	> 15
20m	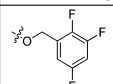	Cl	1.12	> 3
20n	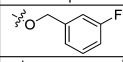	H	0.65	> 15
20o	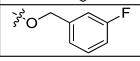	OCH_3	1.88	> 15

[a]All EC_{50} values are ±7%. [b]Concentration giving 50% inhibition of growth of *T brucei brucei* Lister 427 cells

the R^2 position of the headgroup, replacing the chlorine atom of **1** with hydrogen and methoxy groups; these changes also resulted in very modest alterations in antitrypanosomal activity. Interestingly, truncation of the molecule (**20a**) gave potency approximately equal to **10a**, translating to a similar ligand efficiency value (LE of **10a** = 0.14; **20a** = 0.18).[36]

For the next round of analogues, we turned our attention back to further refinement of the tail group region of **1**, performing focused modifications of the 6-aryl position of the quinazoline ring that were designed to evaluate steric requirements as well as the required adornment of polarity in this region of the inhibitor. These compounds (**10k**–**w**) were accessed from the corresponding boronic acids using the route shown in Scheme 1. The larger sulfonamide side chains showed some modest preference for *meta*-substitution (Table 4, entries 1–6), although the methyl sulfones (entries 11–12) showed preference for *para*-substituents. Comparing the sulfonamide substituents, morpholine was preferred over the other heterocycles tested.

A more focused evaluation of linker and regiochemistry is shown in Table 5. Compounds were synthesized from **14** by reaction with the appropriate boronate ester **22**. In the case of the morpholinosulfonamides (entries 1–8), *meta*-substitution is consistently better than *para*; the most potent analogue, NEU617 (**23a**), is directly linked to the aromatic ring (Scheme 4). For piperidinosulfonamides (entries 9–16), the meta preference is less consistent, and none of these analogues show as potent growth inhibition as **23a**. When the tail contains a morpholine (entries 1–8), the linker has little impact on potency (except for **23a**, a clear outlier); all *meta*-substituted analogues are otherwise approximately equipotent. In cases where the morpholine moiety is at the *para*-position, there is little difference resulting from linker variation.

With piperidine-substitution (entries 9–16), it appears that a modest preference exists for the *meta*-substituted amide, with a 6.7-fold loss of activity when moved to the *para* position (compare entries 13 and 14), although the importance of positional substitution is otherwise less for other examples, within ∼2-fold in activity.

Lastly, we sequentially removed the headgroup substituents of **23a**. Removal of one (**23m**) or both (**23n**) halogens afforded an approximately 5-fold reduction in potency, and further truncation (**23o**) significantly reduced antiparasitic activity while restoring HepG2 potency (Table 6).

Noting its potency against *T. brucei* and selectivity over HepG2 cells (Table 5), we advanced **23a** into a mouse oral pharmacokinetic study. Mice were administered a single oral dose (40 mg/kg) of **23a**, and plasma and brain tissue drug levels were measured over 24 h (Supporting Information Figure S1 and Table S6). Although the CNS fraction was low (5%), the plasma levels were in excess of the EC_{50} for >12 h. We determined that **23a** was 99.6% plasma protein bound. However, because trypanosomes are noted for their ability to endocytose host plasma proteins,[29,37,38] we believed that the oral exposure and in vitro potency warranted in vivo efficacy evaluation.

In a test of efficacy in a mouse model of HAT, mice were infected with *T. brucei brucei* CA427 (10^4 cells) and after 24 h were administered a 40 mg/kg dose of **23a** once per day. No

Scheme 3. Synthesis of Headgroup Expansion Set 20[a]

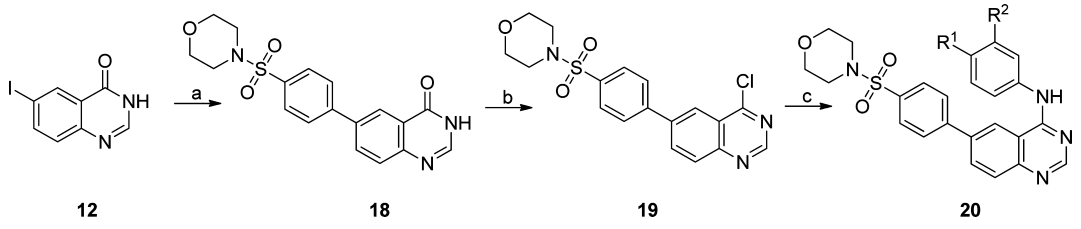

[a]Reagents and conditions: (a) (4-(morpholinosulfonyl)phenyl)boronic acid, $Pd(PPh_3)_4$, 2 M Na_2CO_3, DME, EtOH, 80 °C, 30 h, 85%; (b) thionyl chloride, DMF, 80 °C, 36 h, 66%; (c) Ar-NH_2, 2-propanol, 80 °C, 12 h.

dx.doi.org/10.1021/jm400349k | J. Med. Chem. XXXX, XXX, XXX–XXX

Table 4. *T. brucei* and HepG2 Growth Inhibition Data for Focused Analogues of 10a

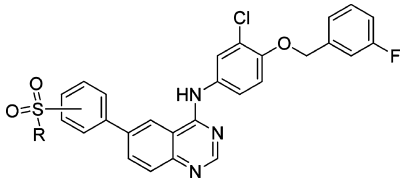

Entry	Compd	position	R_1	Tbb EC_{50} (μM)[a,b]	HepG2 IC_{50} (uM)
1	**10a**	*p*	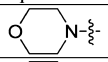	1.39	>15
2	**10k**	*m*	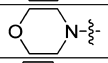	0.33	> 15
3	**10l**	*p*	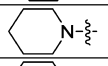	0.32	> 15
4	**10m**	*m*	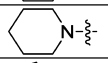	0.46	>15
5	**10n**	*p*		0.35	> 15
6	**10o**	*m*		0.25	> 15
7	**10p**	*p*	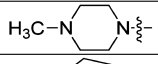	0.53	> 15
8	**10q**	*p*	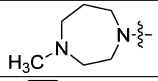	0.81	1.81
9	**10r**	*p*	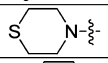	0.47	> 15
10	**10s**	*p*	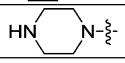	0.28	3.32
11	**10t**	*p*	CH_3	0.90	> 15
12	**10u**	*m*	CH_3	3.21	> 15
13	**10v**	*o*	$N(CH_3)_2$	1.04	> 15
14	**10w**	*o*	$NHC(CH_3)_3$	4.66	nd[c]

[a]All EC_{50} values are ±7%. [b]Concentration giving 50% inhibition of growth of *T brucei brucei* Lister 427 cells. [c]Not determined.

parasites were detected in the blood of the infected mice for 3 days, whereas control mice had trypanosomes in their blood on day 2 postinfection. However drug-related toxicity was observed with **23a** in a multiday regimen at the 40 mg/kg dose. These data point to a need to improve the pharmacokinetic properties of **23a** so that it can be more effective in the mouse model of HAT.

Nonetheless, inspired by these initial results, we adjusted the dosing regimen, opting to administer **23a** at 10 mg/kg twice per day (total dose of 20 mg/kg/day), either orally or intraperitoneally (ip). The results are shown in Figure 1A. We noted three effects: First, ip treatment with **23a** delayed detection of trypanosomes in the blood of infected mice by 24 h. Whereas all control mice had trypanosomes in their blood on day 3, mice treated with **23a** all had parasites in their blood 24 h later, suggestive of either a significant reduction in replication rate (trypanosomes divide every 6 h) or of parasite killing during this initial phase of infection. Second, on day 8 when all untreated mice had died, the mice dosed ip with **23a** were all alive (Figure 1B). In the oral administration experiment, mice died in the same time frame as control mice, suggesting insufficient drug exposure at this dosage. Third, ip administration of **23a** led to better control of infection, leading to a doubling of mouse survival life span from 5 days in the control group to 9 days in **23a**-treated mice.

Although **23a** is structurally similar to **1**, the biological effects of the two compounds are different. Whereas **1** inhibited endocytosis of transferrin in the trypanosome[31] in a manner similar to what we previously observed with tyrphostin,[30] **23a** had no effect on receptor-mediated endocytosis of transferrin. Instead, **23a** affected the cell cycle in ways not observed with **1** (Figure 2).

Trypanosomes possess two DNA-containing organelles (nucleus and kinetoplast (mitochondrial nucleoid)). The kinetoplast and nucleus can be tracked by microscopy during the cell cycle, which begins with trypanosomes harboring one nucleus (1N) and one kinetoplast (1K) (i.e., 1K1N cells).[39,40] A kinetoplast that is replicating its (DNA) (i.e., kDNA) and increasing the organelle's mass is observed as an elongated kinetoplast (1Ke). Fission (segregation) of 1Ke kinetoplasts into two daughter kinetoplasts (2K) inside the same cell is coincident with the nuclear S-phase and produces 2K1N trypanosomes. Mitosis then occurs, yielding trypanosomes containing two kinetoplasts and two nuclei (2K2N). Following cell division, each daughter trypanosome has a 1K1N configuration of the organelles.[41]

After a 7 h incubation with **23a**, the chromosomal DNA profile of *T. brucei* was altered (Figure 2A); the fraction of cells with 2C−4C equivalents of DNA was reduced from 40 to 25%, whereas the proportion of cells with 4C DNA increased from 25% to 40% (Figure 2B). Single cell microscopy studies were performed to determine whether the changes in DNA per cell caused by **23a** (Figure 2B) were reflected in alterations in the number of DNA-containing organelles per cell (Figure 2C). Quantitation of the data obtained in Figure 2C revealed that **23a** reduced the number of cells containing one nucleus (i.e., 1K1N, 1Ke1N) but selectively increased the fraction of a group of cells that are not normally detected in the absence of the

dx.doi.org/10.1021/jm400349k | J. Med. Chem. XXXX, XXX, XXX−XXX

Table 5. Growth Inhibitory Potency of Regiochemical and Linker Analogues of 10

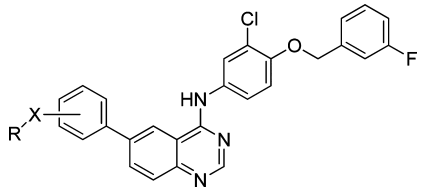

Entry	Compd	R	Regio	X	Tbb EC_{50} (μM)[a,b]	HepG2 IC_{50} (μM)
1	**23a**		m	--	0.042	>20
2	**23b**		p	--	1.91	9.6
3	**23c**		m	CH_2	0.36	nd[c]
4	**23d**		p	CH_2	0.99	12.9
5	**23e**		m	C=O	0.55	nd
6	**23f**		p	C=O	1.21	nd
7	**10k**		m	SO_2	0.33	>20
8	**10a**		p	SO_2	1.39	>20
9	**23g**		m	--	0.76	>15
10	**23h**		p	--	0.38	nd
11	**23i**		m	CH_2	0.65	nd
12	**23j**		p	CH_2	1.5	nd
13	**23k**		m	C=O	0.14	>6
14	**23l**		p	C=O	0.94	nd
15	**10m**		m	SO_2	0.46	>20
16	**10l**		p	SO_2	0.32	>20

[a]All EC_{50} values are ±7%. [b]Concentration giving 50% inhibition of growth of *T brucei brucei* Lister 427 cells. [c]Not determined.

Scheme 4. Synthesis of Analogues 23[a]

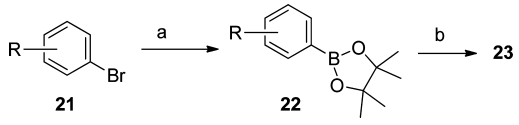

[a]Reagents and conditions: (a) bis(pinacolato)diboron, $PdCl_2(dppf)$-CH_2Cl_2, KOAc, 1,4-dioxane, 80 °C, 12 h, 33–72%; (b) **14**, $Pd(PPh_3)_4$, 2 M Na_2CO_3, DME, EtOH, 80 °C, 12 h.

Table 6. Headgroup Truncation Analogues of 23a

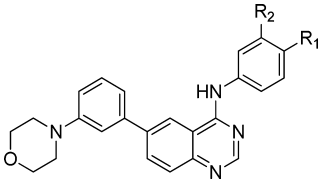

Compound	R^1	R^2	Tbb EC_{50} (μM)[a,b]	HepG2 IC_{50} (μM)	LE
23a	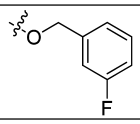	Cl	0.042	>20	0.19
23m	OBn	Cl	0.23	>20	0.18
23n	OBn	H	0.18	>20	0.19
23o	H	H	11	7.02	0.17

[a]All EC_{50} values are ±7%. [b]Concentration giving 50% inhibition of growth of *T brucei brucei* Lister 427 cells.

drug: cells containing two nuclei and one kinetoplast (1K2N) (Figure 2D). This data is consistent with the increase in trypanosomes with 4C equivalent of DNA (Figure 2B). Thus, **23a** blocks duplication of the kinetoplast and arrests cytokinesis without inhibiting division of the trypanosome nucleus.

DISCUSSION AND CONCLUSIONS

While some efforts to find new antitrypanosomal lead compounds involve screening of large compound libraries against cell cultures,[42] these can be complemented with lead discovery programs that target important physiological pathways in the parasite. Further, because many of these pathways employ enzymes of functional similarity to drug targets in humans, a privileged set of starting compounds already exist that can represent useful starting points for lead discovery without massive drug screening initiatives.

In this report, we have described the discovery of potent trypanocidal compounds that are based on established human EGFR inhibitor chemotypes. By starting with such "privileged" lead compounds, we have accelerated our antitrypanosomal lead discovery program by circumventing a need to run high-throughput screens. Indeed, in only a few optimization cycles we have identified a potent chemotype as a lead series for trypanosomiasis. Although compound **23a** has high calculated lipophilicity and molecular weight, its oral bioavailability lent the compound to further assessment in a mouse model of HAT, where we observed modest effects in controlling parasitemia, with concomitant life extension of infected mice. Because the pharmacokinetic experiments suggest acceptable plasma levels in mice following oral dosing, we hypothesize that the high plasma protein binding (99.6%) observed for **23a** is the cause of the lower-than-expected effect on in vivo parasite loads.

Trypanosome physiology analysis indicates that **23a** acts via a mechanism different from **1** and tyrphostin A47. Work is in progress to identify the molecular targets of our lead compound series. Nonetheless, we note that utilization of cell replication assays has led to promising outcomes that are worthy of future lead optimization studies.

Besides working to reduce plasma protein binding, further optimization of **23a** is needed to improve predicted central nervous system exposure. A recent report by Wager et al. described an analysis that correlated compound properties to CNS exposure using data for both experimental and marketed drugs[43] and devised a scoring paradigm for prediction of CNS exposure.[44] This protocol, termed multiparameter optimization, or MPO, allows prediction of likely CNS exposure for a given compound based on how closely it meets desired property ranges for MW, cLogP, Log *D*, pK_a, and TPSA with a maximal MPO score of 6.0, and compounds >4.0 predicted to be CNS-penetrant. As shown in Table 7, compound **23a** has significant shortcomings in terms of properties that have been shown relevant to CNS activity, particularly due to high calculated lipophilicity (cLogP, cLogD = 7.1) and molecular weight (541 Da). Future efforts will be focused on reduction of molecular size and lipophilicity to improve the likelihood of CNS penetration, a pivotal requirement for any new therapeutic for HAT.

In summary, we have identified a potent trypanosomal growth inhibitor (**23a**) based on the 6-furanyl 4-anilinoquinazoline scaffold of **1**. The lead displays good selectivity over HepG2 cells, is orally bioavailable, and is modestly efficacious in a mouse model of HAT, such that it meets "Lead Criteria" as defined by The Special Programme for Research and Training in Tropical Diseases (TDR).[10] Further optimization of this

dx.doi.org/10.1021/jm400349k | J. Med. Chem. XXXX, XXX, XXX–XXX

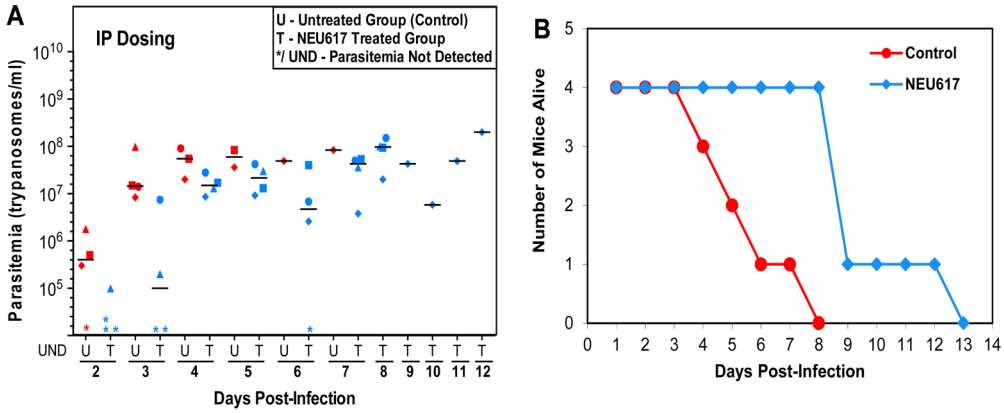

Figure 1. Assessment of **23a** in a mouse model of human African trypanosomiasis. Parasitemia was measured each day in untreated (U, red) and treated (T, blue) mice (20 mg/kg).

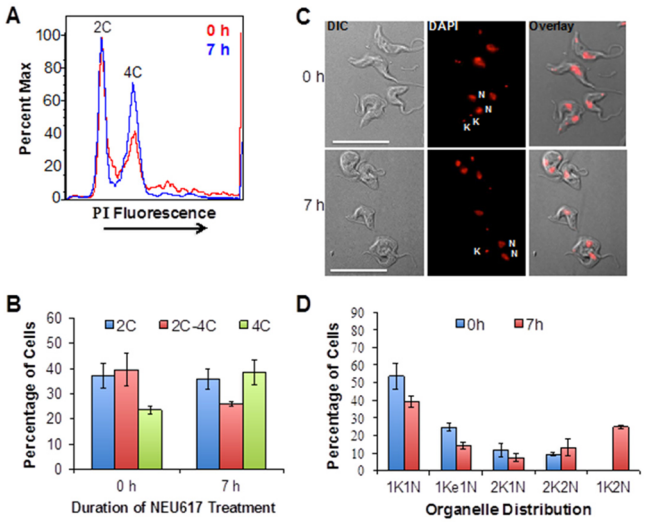

Figure 2. Effects of **23a** on the cell cycle of the trypanosome. (A) **23a**-treated or control trypanosomes were analyzed by flow cytometry (10000 events analyzed; see Experimental Section). Propidium iodide (PI) fluorescence is plotted against cell populations. (B) Quantitation of DNA content per cell (calculated with FloJo software). (C) Microscopic analysis of **23a**-treated or untreated trypanosomes after staining with DNA-binding dye DAPI. N, nucleus; K, kinetoplast; DIC, differential interference contrast image. (D) Quantitation of organelle (nucleus (N) or kinetoplast (K)) distribution after **23a** treatment.

Table 7. Desirable Ranges for CNS Penetration and the MPO Scoring for 23a

Prop	Targeted Value	Properties of 23a	MPO Score
cLogP	≤ 3	7.1	0
cLogD	≤ 2	7.1	0
TPSA	40 < X ≤ 90	59.5	1.00
MW	≤ 360	541	0
HBD	≤ 0.5	1	0.8
pKa	≤ 8	3.05	1.0
		MPO score	**2.8**

scaffold for increased effectiveness in the mouse model will be reported in due course. Our ability to (i) identify trypanosome replication inhibitors based on basic biology principles using established kinase drug chemotypes and (ii) perform rapid hit-to-lead medicinal chemistry supports our approach of reoptimizing existing drug scaffolds for antitrypanosome lead discovery.

EXPERIMENTAL SECTION

Chemical Synthesis. Unless otherwise noted, reagents were obtained from Sigma-Aldrich, Inc. (St. Louis, MO) or Frontier Scientific Services, Inc. (Newark, DE) and used as received. Boronic acids and aniline reagents were purchased unless the synthesis is specifically described below. Reaction solvents were purified by passage through alumina columns on a purification system manufactured by Innovative Technology (Newburyport, MA). NMR spectra were obtained with Varian NMR systems operating at 400 or 500 MHz for ^{1}H acquisitions as noted. LCMS analysis was performed using a Waters Alliance reverse-phase HPLC, with single-wavelength UV−visible detector and LCT Premier time-of-flight mass spectrometer (electrospray ionization). All newly synthesized compounds that were submitted for biological testing were deemed >95% pure by LCMS analysis (UV and ESI-MS detection) prior to submission for biological testing. Preparative LCMS was performed on a Waters FractionLynx system with a Waters MicroMass ZQ mass spectrometer (electrospray ionization) and a single-wavelength UV−visible detector, using acetonitrile/water gradients with 0.1% formic acid. Fractions were collected on the basis of triggering using UV and mass detection. Yields reported for products obtained by preparative HPLC represent the amount of pure material isolated; impure fractions were not repurified. Screening data of selected boronates has been made freely available as a shared data set at www.collaborativedrugdiscovery.com.

4-Chloro-6-iodoquinazoline Hydrochloride (13).[45] Yield: 85%. ^{1}H NMR (500 MHz, DMSO-d_6) δ: 8.39 (d, J = 1.95 Hz, 1H), 8.29 (s, 1H), 8.13 (dd, J = 1.95, 8.30 Hz, 1H), 7.49 (d, J = 8.30 Hz, 1H). MS: m/z = 290.83 $(M + H)^+$.

***N*-(3-Chloro-4-((3-fluorobenzyl)oxy)phenyl)-6-iodoquinazolin-4-amine Hydrochloride (14).**[46] Yield: 84%. ^{1}H NMR (500 MHz, DMSO-d_6) δ: 11.21 (br s, 1H), 9.16 (s, 1H), 8.92 (s, 1H), 8.34 (d, J = 8.79 Hz, 1H), 7.93 (d, J = 2.44 Hz, 1H), 7.64−7.68 (m, 2H), 7.46−7.51 (m, 1H), 7.30−7.37 (m, 2H), 7.20 (dt, J = 2.44, 8.79 Hz, 1H), 5.30 (s, 2H). MS: m/z = 505.85 $(M + H)^+$.

Libraries of **10** were synthesized by Suzuki coupling of **14** with respective boronic acid/esters following general procedure A. Into glass vials was combined *N*-(3-chloro-4-((3-fluorobenzyl)oxy)phenyl)-6-iodoquinazolin-4-amine (**14**, 100 μM), boronic acids/esters (120 μmol), and tetrakis(triphenylphosphine)palladium(0) (7 μmol). To the reaction mixture was added 1,2-dimethoxyethane (2 mL), ethanol (1.33 mL), and a 2 M aqueous solution of sodium carbonate (0.301 mL, 600 μM). The vials were capped and shaken at 80 °C for 18 h. The progress of the reaction was followed by LC-MS. Reaction mixture was evaporated to dryness. Crude products were purified using flash column chromatography or by dissolving in DMSO and

dx.doi.org/10.1021/jm400349k | J. Med. Chem. XXXX, XXX, XXX−XXX

purifying by reverse phase HPLC using a gradient of 30−100% acetonitrile in water containing 0.1% formic acid.

***N*-(3-Chloro-4-((3-fluorobenzyl)oxy)phenyl)-6-(4-(morpholinosulfonyl)phenyl)quinazolin-4-amine (10a).** Yield: 48.1%. ^{1}H NMR (500 MHz, DMSO-d_6) δ: 10.00 (s, 1H), 8.92 (d, J = 1.46 Hz, 1H), 8.64 (s, 1H), 8.28 (dd, J = 1.95, 8.79 Hz, 1H), 8.17 (d, J = 8.79 Hz, 2H), 8.04 (d, J = 2.44 Hz, 1H), 7.92 (d, J = 8.79 Hz, 3H), 7.76 (dd, J = 2.45, 8.80 Hz, 1H), 7.46−7.50 (m, 1H), 7.30−7.36 (m, 3H), 7.19−7.23 (m, 1H), 5.28 (s, 2H), 3.66−3.68 (m, 4H), 2.93−2.95 (m, 4H). MS: m/z = 605.2 (M + H)$^+$.

***N*-(3-Chloro-4-((3-fluorobenzyl)oxy)phenyl)-6-(4-methylnaphthalen-1-yl)quinazolin-4-amine (10b).** Yielded 1 mg (2.6%) as a yellow film. ^{1}H NMR (400 MHz, DMSO-d_6) δ: 9.82 (s, 1H), 8.65 (s, 2H), 8.15 (d, J = 8.8 Hz, 1H), 8.03 (d, J = 2.2 Hz, 1H), 7.87−7.96 (m, 2H), 7.81 (d, J = 8.8 Hz, 1H), 7.71−7.76 (m, 1H), 7.63 (t, J = 8.0 Hz, 1H), 7.49−7.57 (m, 2H), 7.42−7.49 (m, 2H), 7.31 (t, J = 6.0 Hz, 2H), 7.25 (d, J = 8.8 Hz, 1H), 7.17 (t, J = 7.3 Hz, 1H), 5.24 (s, 2H), 2.74 (s, 3H). MS: m/z = 520.1 (M + H)$^+$.

4-(4-((3-Chloro-4-((3-fluorobenzyl)oxy)phenyl)amino)-quinazolin-6-yl)-*N*-ethyl-2-fluorobenzamide (10c). Yielded 1 mg (2.4%) as a yellow film. ^{1}H NMR (400 MHz, DMSO-d_6) δ: 9.98 (s, 1H), 8.87 (s, 1H), 8.58−8.61 (s, 1H), 8.35−8.42 (m, 1H), 8.26−8.34 (m, 1H), 8.01 (s, 1H), 7.87 (d, J = 4.4 Hz, 1H), 7.84 (m, 2H), 7.79 (d, J = 8.1 Hz, 1H), 7.70−7.76 (m, 1H), 7.47 (q, J = 7.3 Hz, 1H), 7.32 (dd, J_A = 13.2 Hz, J_B = 7.3 Hz, 3H), 7.18 (t, J = 8.8 Hz, 1H), 5.27 (s, 2H), 3.29 (q, J = 8.0 Hz, 2H), 1.14 (t, J = 7.0 Hz, 3H). MS: m/z = 545.2 (M + H)$^+$.

***N*-(3-Chloro-4-((3-fluorobenzyl)oxy)phenyl)-6-(3-(5-methyl-1,3,4-oxadiazol-2-yl)phenyl)quinazolin-4-amine (10d).** Obtained 1 mg (2.5% yield) as a yellow oil. ^{1}H NMR (400 MHz, DMSO-d_6) δ: 9.09−10.04 (brs, 1H), 8.88 (s, 1H), 8.61 (s, 1H), 8.42 (s, 1H), 8.37 (s, 1H), 8.26 (d, J = 8.8 Hz, 1H), 8.11 (d, J = 8.1 Hz, 1H), 8.0 (m, 2H), 7.89 (d, J = 8.8 Hz, 1H), 7.72−7.81 (m, 2H), 7.43−7.51 (m, 1H), 7.28−7.36 (m, 2H), 7.14−7.22 (m, 1H) 5.26 (s, 2H), 2.65 (s, 3H). MS: m/z = 538.1 (M + H)$^+$.

3-(4-((3-Chloro-4-((3-fluorobenzyl)oxy)phenyl)amino)-quinazolin-6-yl)-*N*-cyclopropylbenzamide (10e). Yielded 0.8 mg (2.0%) as a yellow film. ^{1}H NMR (400 MHz, DMSO-d_6) δ: 10.00 (s, 1H), 8.83 (s, 1H), 8.63 (d, J = 3.7 Hz, 1H), 8.59 (s, 1H), 8.35 (s, 1H), 8.26 (d, J = 5.1 Hz, 1H), 8.22 (s, 1H), 7.97−8.05 (m, 1H), 7.87 (t, J = 8.1 Hz, 2H), 7.74 (dd, J_A = 8.8 Hz, J_B = 2.0 Hz, 1H), 7.63 (t, J = 7.7 Hz, 1H), 7.43−7.52 (m, 1H), 7.25−7.35 (m, 2H), 7.17 (t, J = 8.0 Hz, 1H), 5.27 (s, 2H), 2.85−2.92 (m, 1H), 0.69−0.76 (m, 2H), 0.58−0.65 (m, 2H). MS: m/z = 539.2 (M + H)$^+$.

***N*-(3-Chloro-4-((3-fluorobenzyl)oxy)phenyl)-6-(quinolin-5-yl)quinazolin-4-amine (10f).** Yielded 3.2 mg (8.4%) as a yellow solid. ^{1}H NMR (400 MHz, DMSO-d_6) δ: 9.81 (s, 1H), 8.98 (d, J = 2.9 Hz, 1H), 8.70 (s, 1H), 8.68 (s, 1H), 8.21−8.27 (m, 1H), 8.14 (d, J = 8.1 Hz, 1H), 8.03 (d, J = 2.2 Hz, 1H), 7.95−8.00 (m, 1H), 7.88−7.95 (m, 2H),7.68−7.96 (m, 2H), 7.53−7.59 (dd, J_A = 8.4 Hz, J_B = 4.0 Hz, 1H), 7.46 (q, J = 8.0 Hz, 1H), 7.22−7.33 (m, 3H), 7.17 (t, J = 8.8 Hz, 1H), 5.23 (s, 2H). MS: m/z = 507.2 (M + H)$^+$.

***N*-(3-Chloro-4-((3-fluorobenzyl)oxy)phenyl)-6-(2-phenoxyphenyl)quinazolin-4-amine (10g).** Yielded 1.4 mg (2.4%) as an orange oil. ^{1}H NMR (400 MHz, DMSO-d_6) δ: 9.85 (s, 1H), 8.65 (s, 1H), 8.58 (s, 1H), 8.01−8.06 (m, 2H), 7.72−7.78 (m, 2H), 7.67 (d, J = 6.6 Hz, 1H), 7.42−7.51 (m, 2H), 7.24−7.39 (m, 6H), 7.19 (t, J = 7.3 Hz, 1H), 7.00−7.09 (m, 2H), 6.94 (d, J = 8.1 Hz, 2H), 5.27 (s, 2H). MS: m/z = 548.1 (M + H)$^+$.

6-(Benzo[b]thiopen-2-yl)-*N*-(3-chloro-4-((3-fluorobenzyl)-oxy)phenyl)quinazolin-4-amine (10h). Obtained 5.4 mg (14% yield) as a yellow solid. ^{1}H NMR (400 MHz, DMSO-d_6) δ: 8.75 (s, 1H), 8.15 (t, J = 8.8 Hz, 1H), 8.03 (m, 1H), 7.96 (d, J = 8.8 Hz, 1H), 7.87 (d, J = 2.1 Hz, 2H), 7.82 (d, J = 7.3 Hz, 1H), 7.68 (s, 1H), 7.51−7.59 (m, 1H), 7.49 (s, 1H), 7.32−7.44 (m, 3H), 7.19−7.25 (m, 1H), 6.91−7.09 (m, 2H), 5.27 (s, 2H). MS: m/z = 512.0 (M + H)$^+$.

4-(4-((3-Chloro-4-((3-fluorobenzyl)oxy)phenyl)amino)-quinazolin-6-yl)phenol (10i). Yielded 1 mg (2.4%) as a yellow film. ^{1}H NMR (400 MHz, DMSO-d_6) δ: 10.09 (s, 1H), 8.98 (s, 1H), 8.63 (s, 2H), 8.45 (s, 1H), 8.42 (s, 1H), 8.05 (s, 1H), 7.96 (d, J = 8.8 Hz, 1H), 7.82 (d, J = 9.5 Hz, 1H), 7.43−7.51 (m, 2H), 7.27−7.36 (m, 2H), 7.14−7.22 (m, 1H), 6.66−6.72 (m, 2H), 5.27 (s, 2H). MS: m/z = 472.1 (M + H)$^+$.

5-(4-((3-Chloro-4-((3-fluorobenzyl)oxy)phenyl)amino)-quinazolin-6-yl)pyrimidine-2,4(1*H*,3*H*)-dione (10j). Yielded 2.6 mg (7.1%) as a yellow solid. ^{1}H NMR (400 MHz, DMSO-d_6) δ: 9.76−9.82 (brs, 1H), 8.47−8.59 (m, 2H), 8.30 (s, 1H), 8.04 (m, 2H), 7.81−7.88 (m, 1H), 7,71−7.80 (m. 2H), 7.59−7.67 (m, 1H), 7.43−7.50 (m, 1H), 7.31−7.36 (m, 1H), (m, 7.23−7.31 (m, 2H), 7.18 (t, J = 8.4 Hz, 1H), 5.26 (s, 2H). MS: m/z = 490.0 (M + H)$^+$.

***N*-(3-Chloro-4-((3-fluorobenzyl)oxy)phenyl)-6-(3-(morpholinosulfonyl)phenyl)quinazolin-4-amine (10k).** Yield: 30.4%. ^{1}H NMR (500 MHz, DMSO-d_6) δ: 10.01 (s, 1H), 8.85 (d, J = 1.95 Hz, 1H), 8.63 (s, 1H), 8.24−8.27 (m, 2H), 8.12 (t, J = 1.71 Hz, 1H), 8.03 (d, J = 2.93 Hz, 1H), 7.86−7.92 (m, 2H), 7.80−7.85 (m, 1H), 7.73 (dd, J = 2.44, 8.79 Hz, 1H), 7.46−7.52 (m, 1H), 7.30−7.35 (m, 3H), 7.17−7.22 (m, 1H), 5.28 (s, 2H), 3.66 (t, J = 4.90 Hz, 4H), 2.95 (t, J = 4.40 Hz, 4H). MS: m/z = 605.1 (M + H)$^+$.

***N*-(3-Chloro-4-((3-fluorobenzyl)oxy)phenyl)-6-(4-(piperidin-1-ylsulfonyl)phenyl)quinazolin-4-amine (10l).** Yield: 14.6%. ^{1}H NMR (500 MHz, DMSO-d_6) δ: 10.00 (s, 1H), 8.91 (d, J = 1.46 Hz, 1H), 8.64 (s, 1H), 8.27 (dd, J = 1.95, 8.30 Hz, 1H), 8.14 (d, J = 8.30 Hz, 2H), 8.04 (d, J = 2.93 Hz, 1H), 7.89−7.92 (m, 3H), 7.76 (dd, J = 2.69, 9.03 Hz, 1H), 7.46−7.51 (m, 1H), 7.31−7.36 (m, 3H), 7.20 (dt, J = 2.44, 8.55 Hz, 1H), 5.28 (s, 2H), 2.95−2.98 (m, 4H), 1.55−1.60 (m, 4H), 1.39−1.40 (m, 2H). MS: m/z = 603.2 (M + H)$^+$.

***N*-(3-Chloro-4-((3-fluorobenzyl)oxy)phenyl)-6-(3-(piperidin-1-ylsulfonyl)phenyl)quinazolin-4-amine (10m).** Yield: 24.8%. ^{1}H NMR (500 MHz, DMSO-d_6) δ: 10.01 (s, 1H), 8.84 (d, J = 1.95 Hz, 1H), 8.62 (s, 1H), 8.24 (dd, J = 1.95, 8.79 Hz, 1H), 8.21 (d, J = 7.35 Hz, 1H), 8.11 (t, J = 1.71 Hz, 1H), 8.02 (d, J = 2.44 Hz, 1H), 7.90 (d, J = 8.30 Hz, 1H), 7.82−7.86 (m, 1H), 7.79−7.81 (m, 1H), 7.72 (dd, J = 2.69, 9.03 Hz, 1H), 7.45−7.51 (m, 1H), 7.29−7.36 (m, 3H), 7.19 (dt, J = 2.44, 8.55 Hz, 1H), 5.27 (s, 2H), 2.96 (t, J = 5.4 Hz, 4Hm, 4H), 1.52−1.60 (m, 4H), 1.33−1.40 (m, 2H). MS: m/z = 603.2 (M + H)$^+$.

***N*-(3-Chloro-4-((3-fluorobenzyl)oxy)phenyl)-6-(4-(pyrrolidin-1-ylsulfonyl)phenyl)quinazolin-4-amine (10n).** Yield: 19.6%. ^{1}H NMR (500 MHz, DMSO-d_6) δ: 10.00 (s, 1H), 8.91 (d, J = 1.95 Hz, 1H), 8.63 (s, 1H), 8.27 (dd, J = 1.95, 8.79 Hz, 1H), 8.13 (d, J = 8.30 Hz, 2H), 8.03 (d, J = 2.44 Hz, 1H), 7.98 (d, J = 8.79 Hz, 2H), 7.90 (d, J = 8.79 Hz, 1H), 7.76 (dd, J = 2.44, 8.79 Hz, 1H), 7.45−7.52 (m, 1H), 7.29−7.36 (m, 3H), 7.20 (dt, J = 2.44, 8.55 Hz, 1H), 5.28 (s, 2H), 3.22 (t, J = 6.84 Hz, 4H), 1.66−1.72 (m, 4H). MS: m/z = 589.1 (M + H)$^+$.

***N*-(3-Chloro-4-((3-fluorobenzyl)oxy)phenyl)-6-(3-(pyrrolidin-1-ylsulfonyl)phenyl)quinazolin-4-amine (10o).** Yield: 28.2%. ^{1}H NMR (500 MHz, DMSO-d_6) δ: 10.03 (s, 1H), 8.85 (d, J = 1.46 Hz, 1H), 8.62 (s, 1H), 8.26 (dd, J = 1.95, 8.79 Hz, 1H), 8.18−8.23 (m, 2H), 8.03 (d, J = 2.44 Hz, 1H), 7.88−7.93 (m, 2H), 7.81−7.87 (m, 1H), 7.73 (dd, J = 2.44, 8.79 Hz, 1H), 7.45−7.52 (m, 1H), 7.30−7.37 (m, 3H), 7.20 (dt, J = 2.44, 8.55 Hz, 1H), 5.28 (s, 2H), 3.23 (t, J = 6.84 Hz, 4H), 1.68 (td, J = 3.54, 6.59 Hz, 4H). MS: m/z = 589.2 (M + H)$^+$.

***N*-(3-Chloro-4-((3-fluorobenzyl)oxy)phenyl)-6-(4-((4-methylpiperazin-1-yl)sulfonyl)phenyl)quinazolin-4-amine (10p).** Yield: 30.6%. ^{1}H NMR (500 MHz, DMSO-d_6) δ: 9.95 (s, 1H), 8.87 (d, J = 1.46 Hz, 1H), 8.59 (s, 1H), 8.23 (dd, J = 1.95, 8.79 Hz, 1H), 8.11 (d, J = 8.30 Hz, 2H), 7.99 (d, J = 2.44 Hz, 1H), 7.83−7.90 (m, 3H), 7.71 (dd, J = 2.69, 9.03 Hz, 1H), 7.40−7.47 (m, 1H), 7.25−7.32 (m, 3H), 7.15 (dt, J = 2.44, 8.55 Hz, 1H), 5.23 (s, 2H), 2.91 (br s, 4H), 2.34 (br s, 4H), 2.11 (s, 3H). MS: m/z = 618.2 (M + H)$^+$.

***N*-(3-Chloro-4-((3-fluorobenzyl)oxy)phenyl)-6-(4-((4-methyl-1,4-diazepan-1-yl)sulfonyl)phenyl)quinazolin-4-amine (10q).** Yield: 42.8%. ^{1}H NMR (500 MHz, DMSO-d_6) δ: 10.00 (s, 1H), 8.91 (d, J = 1.95 Hz, 1H), 8.63 (s, 1H), 8.27 (dd, J = 1.95, 8.79 Hz, 1H), 8.12 (d, J = 8.80 Hz, 2H), 8.03 (d, J = 2.44 Hz, 1H), 7.96 (d, J = 8.30 Hz, 2H), 7.90 (d, J = 8.79 Hz, 1H), 7.76 (dd, J = 2.69, 9.03 Hz, 1H), 7.45−7.50 (m, 1H), 7.30−7.36 (m, 3H), 7.20 (dt, J = 2.44, 8.55 Hz, 1H), 5.28 (s, 2H), 3.37−3.39 (m, 2H), 3.34 (t, J = 6.10 Hz, 2H), 2.61−2.64 (m, 2H), 2.54−2.58 (m, 2H), 2.28 (s, 3H), 1.74−1.80 (m, 2H). MS: m/z = 632.2 (M + H)$^+$.

***N*-(3-Chloro-4-((3-fluorobenzyl)oxy)phenyl)-6-(4-(thiomorpholinosulfonyl)phenyl)quinazolin-4-amine (10r).**

dx.doi.org/10.1021/jm400349k | J. Med. Chem. XXXX, XXX, XXX−XXX

Yield: 5.6%. ^{1}H NMR (500 MHz, DMSO-d_6) δ: 10.00 (s, 1H), 8.92 (d, J = 1.47 Hz, 1H), 8.64 (s, 1H), 8.28 (dd, J = 1.95, 8.79 Hz, 1H), 8.16 (d, J = 8.79 Hz, 2H), 8.04 (d, J = 2.44 Hz, 1H), 7.89−7.95 (m, 3H), 7.76 (dd, J = 2.45, 8.80 Hz, 1H), 7.46−7.52 (m, 1H), 7.30−7.37 (m, 3H), 7.20 (dt, J = 2.20, 8.67 Hz, 1H), 5.28 (s, 2H), 3.28 (t, J = 4.35 Hz, 4H), 2.71 (t, J = 5.35 Hz, 4H). MS: m/z = 621.2 $(M + H)^+$.

***N*-(3-Chloro-4-((3-fluorobenzyl)oxy)phenyl)-6-(4-(piperazin-1-ylsulfonyl)phenyl)quinazolin-4-amine (10s).** To glass vials was weighed 46 mg of **14** (0.085 mmoL) and *tert*-butyl 4-((4-(4,4,5,5-tetramethyl-1,3,2-dioxaborolan-2-yl)phenyl)sulfonyl)piperazine-1-carboxylate (38.4 mg 0.085 mmol) and tetrakis(triphenylphosphine)-palladium(0) (0.006 mmol). To the reaction mixture was added 1,2-dimethoxyethane (0.4 mL), ethanol (0.3 mL), and a 2 M aqueous solution of sodium carbonate (0.255 mL, 0.51 mmol). The vials were capped and shaken at 85 °C for 12 h, and progress of the reaction was monitored by LC-MS. The reaction mixture was evaporated to dryness, and the residue was dissolved in DMSO and purified by reverse phase HPLC using a gradient of 5−100% acetonitrile in water containing 0.1% formic acid, providing the Boc-protected compound in 23.7% yield. ^{1}H NMR (500 MHz, DMSO-d_6) δ: 9.99 (s, 1H), 8.91 (d, J = 1.95 Hz, 1H), 8.64 (s, 1H), 8.28 (dd, J = 1.95, 8.79 Hz, 1H), 8.16 (d, J = 8.79 Hz, 2H), 8.04 (d, J = 2.44 Hz, 1H), 7.89−7.93 (m, 3H), 7.76 (dd, J = 2.44, 8.79 Hz, 1H), 7.46−7.52 (m, 1H), 7.30−7.36 (m, 3H), 7.20 (dt, J = 2.44, 8.79 Hz, 1H), 5.28 (s, 2H), 3.41−3.46 (m, 4H), 2.94 (t, J = 4.64 Hz, 4H), 1.34 (s, 9H). MS: m/z = 704.3 $(M + H)^+$. To a solution of this compound (0.015 mmol) in 0.4 mL of dichloromethane was added trifluoroacetic acid (200 μmol, 0.154 mL). The reaction mixture was stirred for 12 h at 25 °C. Volatiles were removed in vacuo, and the crude product was triturated with hexanes to afford a crude solid that was purified via flash column chromatography (0−10% MeOH−DCM) to afford the desired compound **10t**. Yield: 78%. ^{1}H NMR (500 MHz, DMSO-d_6) δ: 9.01 (s, 1H), 8.80 (br s, 1H), 8.59 (br s, 2H), 8.39 (d, J = 7.81 Hz, 1H), 8.22 (d, J = 8.30 Hz, 2H), 7.92−8.03 (m, 4H), 7.72 (dd, J = 2.44, 8.79 Hz, 1H), 7.47−7.52 (m, 1H), 7.32−7.37 (m, 3H), 7.21 (dt, J = 2.20, 8.67 Hz, 1H), 5.31 (s, 2H), 3.25 (br s, 4H), 3.18 (br s, 4H). MS: m/z = 604.2 $(M + H)^+$.

***N*-(3-Chloro-4-((3-fluorobenzyl)oxy)phenyl)-6-(4-(methylsulfonyl)phenyl)quinazolin-4-amine (10t).** Yield: 31.8%. ^{1}H NMR (500 MHz, DMSO-d_6) δ: 10.00 (s, 1H), 8.92 (d, J = 1.95 Hz, 1H), 8.64 (s, 1H), 8.29 (dd, J = 1.95, 8.79 Hz, 1H), 8.14 (d, J = 8.80 Hz, 2H), 8.11 (d, J = 8.30 Hz, 2H), 8.03 (d, J = 2.44 Hz, 1H), 7.92 (d, J = 8.79 Hz, 1H), 7.76 (dd, J = 2.44, 8.79 Hz, 1H), 7.45−7.53 (m, 1H), 7.31−7.37 (m, 3H), 7.20 (dt, J = 2.20, 8.42 Hz, 1H), 5.28 (s, 2H), 3.31 (s, 3H). MS: m/z = 534.1 $(M + H)^+$.

***N*-(3-Chloro-4-((3-fluorobenzyl)oxy)phenyl)-6-(3-(methylsulfonyl)phenyl)quinazolin-4-amine (10u).** Yield: 34.9%. ^{1}H NMR (500 MHz, DMSO-d_6) δ: 10.02 (s, 1H), 8.88 (s, 1H), 8.63 (s, 1H), 8.38 (s, 1H), 8.30 (dd, J = 1.46, 8.79 Hz, 1H), 8.25 (d, J = 8.30 Hz, 1H), 7.99−8.06 (m, 2H), 7.92 (d, J = 8.79 Hz, 1H), 7.84−7.87 (m, 1H), 7.74 (dd, J = 2.44, 8.79 Hz, 1H), 7.45−7.53 (m, 1H), 7.30−7.36 (m, 3H), 7.20 (dt, J = 1.71, 8.67 Hz, 1H), 5.28 (s, 2H), 3.35 (s, 3H). MS: m/z = 534.2 $(M + H)^+$.

2-(4-((3-Chloro-4-((3-fluorobenzyl)oxy)phenyl)amino)-quinazolin-6-yl)-*N*,*N*-dimethylbenzenesulfonamide (10v). Yield: 35%. ^{1}H NMR (500 MHz, DMSO-d_6) δ: 9.78 (s, 1H), 8.65 (s, 1H), 8.52 (d, J = 0.98 Hz, 1H), 8.06 (d, J = 2.44 Hz, 1H), 8.01 (dd, J = 0.98, 7.81 Hz, 1H), 7.83 (dt, J = 1.46, 9.03 Hz, 1H), 7.76−7.81 (m, 3H), 7.72 (dt, J = 1.22, 7.69 Hz, 1H), 7.54 (dd, J = 0.98, 7.81 Hz, 1H), 7.45−7.50 (m, 1H), 7.30−7.34 (m, 2H), 7.27 (d, J = 8.79 Hz, 1H), 7.19 (dt, J = 2.44, 8.55 Hz, 1H), 5.26 (s, 2H), 2.45 (s, 6H). MS: m/z = 563.2 $(M + H)^+$.

***N*-(*tert*-Butyl)-2-(4-((3-chloro-4-((3-fluorobenzyl)oxy)-phenyl)amino)quinazolin-6-yl)benzenesulfonamide (10w).** Yield: 12.5%. ^{1}H NMR (500 MHz, DMSO-d_6) δ: 9.79 (s, 1H), 8.64 (s, 1H), 8.53 (d, J = 1.95 Hz, 1H), 8.11 (dd, J = 1.22, 8.06 Hz, 1H), 8.05 (d, J = 2.44 Hz, 1H), 7.86 (dd, J = 1.71, 8.55 Hz, 1H), 7.70−7.79 (m, 3H), 7.63−7.67 (m, 1H), 7.45−7.50 (m, 2H), 7.30−7.35 (m, 2H), 7.27 (d, J = 9.28 Hz, 1H), 7.19 (dt, J = 2.44, 8.55 Hz, 1H), 6.90 (s, 1H), 5.26 (s, 2H), 1.04 (s, 9H). MS: m/z = 591.2$(M + H)^+$.

***N*-(3-Chloro-4-((3-fluorobenzyl)oxy)phenyl)-6-(3-morpholinophenyl)quinazolin-4-amine (23a).** Yield: 38%. ^{1}H NMR (500 MHz, DMSO-d_6) δ: 9.90 (s, 1H), 8.76 (d, J = 1.95 Hz, 1H), 8.60 (s, 1H), 8.18 (dd, J = 1.71, 8.55 Hz, 1H), 8.04 (d, J = 2.93 Hz, 1H), 7.84 (d, J = 8.79 Hz, 1H), 7.76 (dd, J = 2.44, 8.79 Hz, 1H), 7.45−7.51 (m, 1H), 7.39−7.42 (m, 1H), 7.28−7.35 (m, 5H), 7.19 (dt, J = 2.44, 8.55 Hz, 1H), 7.03 (dd, J = 1.95, 8.30 Hz, 1H), 5.27 (s, 2H), 3.79 (t, J = 4.9 Hz, 4H), 3.24 (t, J = 4.86 Hz, 4H). MS: m/z = 541.2 $(M + H)^+$.

***N*-(3-Chloro-4-((3-fluorobenzyl)oxy)phenyl)-6-(4-morpholinophenyl)quinazolin-4-amine (23b).** Yield: 35.2%. ^{1}H NMR (500 MHz, DMSO-d_6) δ: 9.87 (s, 1H), 8.72 (d, J = 1.95 Hz, 1H), 8.55 (s, 1H), 8.16 (dd, J = 1.95, 8.79 Hz, 1H), 8.03 (d, J = 2.93 Hz, 1H), 7.78−7.82 (m, 3H), 7.76 (dd, J = 2.44, 8.79 Hz, 1H), 7.45−7.51 (m, 1H), 7.28−7.35 (m, 3H), 7.19 (dt, J = 2.69, 8.67 Hz, 1H), 7.11 (d, J = 8.79 Hz, 2H), 5.27 (s, 2H), 3.76−3.80 (m, 4H), 3.19−3.23 (m, 4H). MS: m/z = 541.04 $(M + H)^+$.

***N*-(3-Chloro-4-((3-fluorobenzyl)oxy)phenyl)-6-(3-(morpholinomethyl)phenyl)quinazolin-4-amine (23c).** Yield: 54.5%. ^{1}H NMR (500 MHz, DMSO-d_6) δ: 9.92 (s, 1H), 8.77 (s, 1H), 8.59 (s, 1H), 8.15 (d, J = 8.79 Hz, 1H), 8.03 (d, J = 1.95 Hz, 1H), 7.85 (d, J = 8.79 Hz, 1H), 7.72−7.80 (m, 3H), 7.43−7.54 (m, 2H), 7.39 (d, J = 7.32 Hz, 1H), 7.25−7.35 (m, 3H), 7.14−7.22 (m, 1H), 5.26 (s, 2H), 3.52−3.68 (m, 6H), 2.40 (br s, 4H). MS: m/z = 554.3 $(M)^+$.

***N*-(3-Chloro-4-((3-fluorobenzyl)oxy)phenyl)-6-(4-(morpholinomethyl)phenyl)quinazolin-4-amine (23d).** Yield: 36.8%. ^{1}H NMR (500 MHz, DMSO-d_6) δ: 9.92 (s, 1H), 8.80 (d, J = 1.95 Hz, 1H), 8.60 (s, 1H), 8.20 (dd, J = 1.95, 8.79 Hz, 1H), 8.04 (d, J = 2.44 Hz, 1H), 7.84−7.87 (m, 3H), 7.77 (dd, J = 2.69, 9.03 Hz, 1H), 7.46−7.54 (m, 3H), 7.28−7.36 (m, 3H), 7.20 (dt, J = 1.95, 8.55 Hz, 1H), 5.28 (s, 2H), 3.61 (t, J = 4.64 Hz, 4H), 3.56 (s, 2H), 2.40 (br s, 4H). MS: m/z = 555.2 $(M + H)^+$.

(3-(4-((3-Chloro-4-((3-fluorobenzyl)oxy)phenyl)amino)-quinazolin-6-yl)phenyl)(morpholino)methanone (23e). Yield: 53.2%. ^{1}H NMR (500 MHz, DMSO-d_6) δ: 9.99 (br s, 1H), 8.83 (d, J = 1.46 Hz, 1H), 8.61 (s, 1H), 8.23 (dd, J = 1.46, 8.79 Hz, 1H), 8.01 (d, J = 2.44 Hz, 1H), 7.97 (d, J = 7.81 Hz, 1H), 7.92 (s, 1H), 7.86 (d, J = 8.79 Hz, 1H), 7.73 (dd, J = 2.44, 8.79 Hz, 1H), 7.63 (t, J = 7.81 Hz, 1H), 7.47 (q, J = 7.65 Hz, 2H), 7.26−7.36 (m, 3H), 7.18 (dt, J = 2.20, 8.67 Hz, 1H), 5.26 (s, 2H), 3.20−3.78 (m, 8H). MS: m/z = 568.2 $(M)^+$.

(4-(4-((3-Chloro-4-((3-fluorobenzyl)oxy)phenyl)amino)-quinazolin-6-yl)phenyl)(morpholino)methanone (23f). Yield: 58.9%. ^{1}H NMR (500 MHz, DMSO-d_6) δ: 9.93 (br s, 1H), 8.84 (br s, 1H), 8.60 (s, 1H), 8.21 (d, J = 8.30 Hz, 1H), 7.93−8.05 (m, 3H), 7.86 (d, J = 8.30 Hz, 1H), 7.76 (d, J = 7.81 Hz, 1H), 7.60 (d, J = 7.81 Hz, 2H), 7.43−7.51 (m, 1H), 7.26−7.36 (m, 3H), 7.18 (t, J = 8.06 Hz, 1H), 5.26 (s, 2H), 3.37−3.80 (m, 8H). MS: m/z = 568.2183 (M).

***N*-(3-Chloro-4-((3-fluorobenzyl)oxy)phenyl)-6-(3-(piperidin-1-yl)phenyl)quinazolin-4-amine (23g).** Yield: 21%. ^{1}H NMR (500 MHz, DMSO-d_6) δ: 9.90 (s, 1H), 8.74 (d, J = 1.95 Hz, 1H), 8.58 (s, 1H), 8.16 (dd, J = 1.71, 8.55 Hz, 1H), 8.03 (d, J = 2.44 Hz, 1H), 7.83 (d, J = 8.79 Hz, 1H), 7.75 (dd, J = 2.44, 8.79 Hz, 1H), 7.44−7.51 (m, 1H), 7.27−7.39 (m, 5H), 7.23 (d, J = 7.81 Hz, 1H), 7.19 (dt, J = 2.44, 8.55 Hz, 1H), 7.00 (dd, J = 1.95, 8.30 Hz, 1H), 5.27 (s, 2H), 3.23−3.27 (m, 4H), 1.64−1.69 (m, 4H), 1.53−1.59 (m, 2H). MS: m/z = 539.16 $(M + H)^+$.

***N*-(3-Chloro-4-((3-fluorobenzyl)oxy)phenyl)-6-(4-(piperidin-1-yl)phenyl)quinazolin-4-amine (23h).** Yield: 41.4%. ^{1}H NMR (500 MHz, DMSO-d_6) δ: 9.87 (s, 1H), 8.69 (d, J = 0.98 Hz, 1H), 8.55 (s, 1H), 8.12 (dd, J = 1.71, 8.55 Hz, 1H), 8.03 (d, J = 2.44 Hz, 1H), 7.72−7.81 (m, 4H), 7.43−7.51 (m, 1H), 7.25−7.37 (m, 3H), 7.18 (dt, J = 2.44, 8.55 Hz, 1H), 7.06 (d, J = 8.79 Hz, 2H), 5.26 (s, 2H), 3.18−3.26 (m, 4H), 1.49−1.70 (m, 6H). MS: m/z = 532.4 $(M)^+$.

***N*-(3-Chloro-4-((3-fluorobenzyl)oxy)phenyl)-6-(3-(piperidin-1-ylmethyl)phenyl)quinazolin-4-amine (23i).** Yield: 66.7%. ^{1}H NMR (500 MHz, DMSO-d_6) δ: 9.91 (br s, 1H), 8.81 (d, J = 1.95 Hz, 1H), 8.60 (s, 1H), 8.19 (dd, J = 1.95, 8.79 Hz, 1H), 8.01 (d, J = 2.93 Hz, 1H), 7.87−7.97 (m, 3H), 7.74 (dd, J = 2.90, 9.25 Hz, 1H), 7.63 (t, J = 7.57 Hz, 1H), 7.52 (d, J = 7.32 Hz, 1H), 7.46 (dt, J = 6.35, 8.06 Hz,

dx.doi.org/10.1021/jm400349k | J. Med. Chem. XXXX, XXX, XXX−XXX

1H), 7.26−7.35 (m, 3H), 7.17 (dt, J = 2.44, 8.55 Hz, 1H), 5.25 (s, 2H), 4.22 (br s, 2H), 3.00 (d, J = 5.86 Hz, 4H), 1.42−1.77 (m, 6H). MS: m/z = 552.3 $(M)^+$.

***N*-(3-Chloro-4-((3-fluorobenzyl)oxy)phenyl)-6-(4-(piperidin-1-ylmethyl)phenyl)quinazolin-4-amine (23j).** Yield: 52.3%. ^{1}H NMR (500 MHz, DMSO-d_6) δ: 9.89 (br s, 1H), 8.80 (d, J = 1.46 Hz, 1H), 8.58 (s, 1H), 8.19 (dd, J = 1.95, 8.79 Hz, 1H), 8.01 (d, J = 2.44 Hz, 1H), 7.90 (d, J = 8.30 Hz, 2H), 7.85 (d, J = 8.79 Hz, 1H), 7.74 (dd, J = 2.44, 8.79 Hz, 1H), 7.56 (d, J = 8.30 Hz, 2H), 7.41−7.50 (m, 1H), 7.25−7.35 (m, 3H), 7.17 (dt, J = 2.20, 8.67 Hz, 1H), 5.25 (s, 2H), 3.93 (br s, 2H), 2.74 (br s, 4H), 1.56−1.69 (m, 4H), 1.45 (br s, 2H). MS: m/z = 552.3 $(M)^+$.

(3-(4-((3-Chloro-4-((3-fluorobenzyl)oxy)phenyl)amino)-quinazolin-6-yl)phenyl)(piperidin-1-yl)methanone (23k). Yield: 66.3%. ^{1}H NMR (500 MHz, DMSO-d_6) δ: 8.91 (s, 1H), 8.76 (br s, 1H), 8.35 (d, J = 9.28 Hz, 1H), 7.96−8.00 (m, 2H), 7.87−7.93 (m, 2H), 7.70 (dd, J = 2.45, 8.80 Hz, 1H), 7.59−7.65 (m, 2H), 7.44−7.52 (m, 2H), 7.32−7.36 (m, 3H), 7.20 (dt, J = 2.44, 8.79 Hz, 1H), 5.30 (s, 2H), 3.65 (br s, 3H), 1.41−1.70 (m, 7H). MS: m/z = 567.3 $(M + H)^+$.

(4-(4-((3-Chloro-4-((3-fluorobenzyl)oxy)phenyl)amino)-quinazolin-6-yl)phenyl)(piperidin-1-yl)methanone (23l). Yield: 73.3%. ^{1}H NMR (500 MHz, DMSO-d_6) δ: 9.93 (s, 1H), 8.83 (s, 1H), 8.59 (s, 1H), 8.21 (dd, J = 1.95, 8.30 Hz, 1H), 8.01 (d, J = 2.44 Hz, 1H), 7.93 (d, J = 8.30 Hz, 2H), 7.86 (d, J = 8.79 Hz, 1H), 7.74 (dd, J = 2.44, 8.79 Hz, 1H), 7.53 (d, J = 8.30 Hz, 3H), 7.43−7.49 (m, 1H), 7.27−7.34 (m, 3H), 7.17 (dt, J = 1.95, 8.55 Hz, 1H), 5.25 (s, 2H), 3.60 (br s, 2H), 1.38−1.67 (m, 7H). MS: m/z = 567.3 $(M + H)^+$.

***N*-(4-(Benzyloxy)-3-chlorophenyl)-6-(3-morpholinophenyl)-quinazolin-4-amine (23m).** Yield: 38%. ^{1}H NMR (500 MHz, DMSO-d_6) δ: 9.88 (s, 1H), 8.75 (d, J = 1.95 Hz, 1H), 8.58 (s, 1H), 8.18 (dd, J = 1.95, 8.79 Hz, 1H), 8.01 (d, J = 2.93 Hz, 1H), 7.84 (d, J = 8.30 Hz, 1H), 7.74 (dd, J = 2.69, 9.03 Hz, 1H), 7.50 (d, J = 7.32 Hz, 2H), 7.39−7.45 (m, 3H), 7.33−7.37 (m, 2H), 7.30 (d, J = 8.79 Hz, 2H), 7.03 (dd, J = 1.95, 8.30 Hz, 1H), 5.24 (s, 2H), 3.77−3.81 (m, 4H), 3.22−3.25 (m, 4H). MS: m/z = 523.07 $(M + H)^+$.

***N*-(4-(Benzyloxy)phenyl)-6-(3-morpholinophenyl)-quinazolin-4-amine (23n).** Yield: 18%. ^{1}H NMR (500 MHz, DMSO-d_6) δ: 9.84 (s, 1H), 8.76 (d, J = 1.46 Hz, 1H), 8.51 (s, 1H), 8.16 (dd, J = 1.95, 8.79 Hz, 1H), 7.81 (d, J = 8.30 Hz, 1H), 7.68 (d, J = 9.30 Hz, 2H), 7.48 (d, J = 7.32 Hz, 2H), 7.38−7.43 (m, 3H), 7.28−7.37 (m, 3H), 7.07 (d, J = 8.80 Hz, 2H), 7.02 (dd, J = 1.95, 7.80 Hz, 1H), 5.14 (s, 2H), 3.78 (t, J = 4.87 Hz, 4H), 3.24 (t, J = 4.87 Hz, 4H). MS: m/z = 489.11 $(M + H)^+$.

6-(3-Morpholinophenyl)-*N*-phenylquinazolin-4-amine (23o). Yield: 57.5%. ^{1}H NMR (500 MHz, DMSO-d_6) δ: 9.92 (s, 1H), 8.80 (d, J = 1.46 Hz, 1H), 8.58 (s, 1H), 8.19 (dd, J = 1.95, 8.79 Hz, 1H), 7.82−7.87 (m, 3H), 7.39−7.45 (m, 3H), 7.36 (d, J = 2.44 Hz, 1H), 7.30−7.33 (m, 1H), 7.15−7.18 (m, 1H), 7.03 (dd, J = 2.20, 8.06 Hz, 1H), 3.79 (t, J = 4.85 Hz, 4H), 3.24 (t, J = 4.85 Hz, 4H). MS: m/z = 383.06 $(M + H)^+$.

Aniline Synthesis. Anilines **17** were synthesized using general procedure B. In a 20 mL glass vial, a solution of substituted 4-nitrophenol (1.5 mmol) in 5 mL of acetonitrile was combined with potassium carbonate (3 mmol) and the appropriate benzyl bromide (1.5 mmol) at 25 °C. The reaction mixture was stirred at 50 °C for 12 h. After completion of the alkylation reaction, the reaction mixture was triturated with 10 mL of 10% MeOH/DCM and was filtered through a silica gel plug. The organic filtrate was evaporated and redissolved in 5 mL of MeOH:H_2O (5:1). To this solution was added zinc (0.29 g, 4.5 mmol), followed by ammonium chloride (0.48 g, 9 mmol) at 25 °C. The temperature was raised to 50 °C, and the stirring was continued for 6 h. Progress of the reaction was followed by LC-MS. Upon completion of the reaction, 15 mL of DCM:MeOH (1:1) was added to the reaction mixture and inorganic residues were removed by filtration. The filtrate was evaporated, and the residue was purified via flash chromatography (0−50% EtOAc/hexanes) to afford the desired substituted anilines.

4-(Benzyloxy)-3-chloroaniline (17e). Yield: 24.3%. ^{1}H NMR (500 MHz, $CDCl_3$) δ: 7.47 (d, J = 7.32 Hz, 2H), 7.37−7.41 (m, 2H), 7.30−7.35 (m, 1H), 6.81 (d, J = 8.79 Hz, 1H), 6.76 (d, J = 2.93 Hz, 1H), 6.51 (dd, J = 2.69, 8.55 Hz, 1H), 5.06 (s, 2H), 3.49 (br s, 2H). MS: m/z = 234.02 $(M + H)^+$.

4-((3-Bromobenzyl)oxy)-3-chloroaniline (17f). Yield: 25%. ^{1}H NMR (500 MHz, $CDCl_3$) δ: 7.62 (s, 1H), 7.45 (d, J = 8.30 Hz, 1H), 7.39 (d, J = 7.81 Hz, 1H), 7.22−7.26 (m, 1H), 6.75−6.80 (m, 2H), 6.52 (dd, J = 2.93, 8.79 Hz, 1H), 5.01 (s, 2H), 3.52 (br s, 2H). MS: m/z = 311.89 $(M + H)^+$.

3-Chloro-4-((3-chlorobenzyl)oxy)aniline (17g). Yield: 38%. ^{1}H NMR (500 MHz, $CDCl_3$) δ: 7.47 (s, 1H), 7.29−7.36 (m, 3H), 6.78 (d, J = 8.30 Hz, 1H), 6.75 (d, J = 2.44 Hz, 1H), 6.50 (dd, J = 2.93, 8.79 Hz, 1H), 5.01 (s, 2H), 3.52 (br s, 2H). MS: m/z = 267.96 $(M + H)^+$.

3-Chloro-4-((2,3-difluorobenzyl)oxy)aniline (17h). Yield: 31%. ^{1}H NMR (500 MHz, $CDCl_3$) δ: 7.35 (t, J = 6.59 Hz, 1H), 7.07−7.16 (m, 2H), 6.83 (d, J = 8.79 Hz, 1H), 6.75 (d, J = 2.93 Hz, 1H), 6.52 (dd, J = 2.69, 8.55 Hz, 1H), 5.12 (s, 2H), 3.51 (br s, 2H). MS: m/z = 270.0 $(M + H)^+$.

3-Chloro-4-((2-fluorobenzyl)oxy)aniline (17i). Yield: 37%. ^{1}H NMR (500 MHz, $CDCl_3$) δ: 7.58 (dt, J = 1.71, 7.45 Hz, 1H), 7.27−7.32 (m, 1H), 7.16 (dt, J = 0.98, 7.57 Hz, 1H), 7.04−7.08 (m, 1H), 6.83 (d, J = 8.79 Hz, 1H), 6.75 (d, J = 2.93 Hz, 1H), 6.51 (dd, J = 2.69, 8.55 Hz, 1H), 5.12 (s, 2H), 3.50 (br s, 2H). MS: m/z = 251.99 $(M + H)^+$.

3-Chloro-4-((4-fluorobenzyl)oxy)aniline (17j). Yield: 22%. ^{1}H NMR (500 MHz, $CDCl_3$) δ: 7.40−7.44 (m, 2H), 7.03−7.10 (m, 2H), 6.78 (d, J = 8.79 Hz, 1H), 6.75 (d, J = 2.44 Hz, 1H), 6.50 (dd, J = 2.93, 8.79 Hz, 1H), 5.00 (s, 2H), 3.50 (br s, 2H). MS: m/z = 252.0 $(M + H)^+$.

3-Chloro-4-((3-methoxybenzyl)oxy)aniline (17k). Yield: %. ^{1}H NMR (500 MHz, $CDCl_3$) δ: 7.27−7.32 (m, 1H), 7.01−7.05 (m, 2H), 6.86 (dd, J = 2.69, 8.06 Hz, 1H), 6.79 (d, J = 8.79 Hz, 1H), 6.74 (d, J = 2.93 Hz, 1H), 6.49 (dd, J = 2.45, 8.80 Hz, 1H), 5.04 (s, 2H), 3.83 (s, 3H), 3.44 (br s, 2H). MS: m/z = 264.01 $(M + H)^+$.

3-Chloro-4-((3-fluoro-4-(trifluoromethyl)benzyl)oxy)aniline (17l). Yield: 35.2%. ^{1}H NMR (500 MHz, $CDCl_3$) δ: 7.60 (t, J = 7.81 Hz, 1H), 7.29−7.36 (m, 2H), 6.77 (d, J = 4.39 Hz, 1H), 6.76 (d, J = 1.47 Hz, 1H), 6.51 (dd, J = 2.93, 8.79 Hz, 1H), 5.06 (s, 2H), 3.54 (br s, 2H). MS: m/z = 319.93 $(M + H)^+$.

3-Chloro-4-((2,3,5-trifluorobenzyl)oxy)aniline (17m). Yield: 22%. ^{1}H NMR (500 MHz, $CDCl_3$) δ: 7.13−7.18 (m, 1H), 6.85−6.93 (m, 1H), 6.81 (d, J = 8.30 Hz, 1H), 6.76 (d, J = 2.93 Hz, 1H), 6.53 (dd, J = 2.93, 8.79 Hz, 1H), 5.09 (s, 2H), 3.54 (br s, 2H). MS: m/z = 287.96 $(M + H)^+$.

4-((3-Fluorobenzyl)oxy)aniline (17n). Yield: 28%. ^{1}H NMR (500 MHz, $CDCl_3$) δ: 7.34 (m, 1H), 7.14−7.21 (m, 2H), 7.01 (dt, J = 2.44, 8.55 Hz, 1H), 6.81 (d, J = 8.30 Hz, 2H), 6.64 (d, J = 8.30 Hz, 2H), 4.99 (s, 2H), 3.32 (br s, 2H). MS: m/z = 218.07 $(M + H)^+$.

4-((3-Fluorobenzyl)oxy)-3-methoxyaniline (17o). Yield: 7.52%. ^{1}H NMR (500 MHz, $CDCl_3$) δ: 7.28−7.33 (m, 1H), 7.14−7.21 (m, 2H), 6.97 (dt, J = 2.20, 8.67 Hz, 1H), 6.70 (d, J = 8.30 Hz, 1H), 6.32 (d, J = 2.93 Hz, 1H), 6.16 (dd, J = 2.69, 8.55 Hz, 1H), 5.02 (s, 2H), 3.84 (s, 3H), 3.51 (br s, 2H). MS: m/z = 248.06 $(M + H)^+$.

6-(4-(Morpholinosulfonyl)phenyl)quinazolin-4(3*H*)-one (18). A mixture of 6-iodoquinazolin-4(3*H*)-one (4.5 g, 16.54 mmol), (4-(morpholinosulfonyl)phenyl)boronic acid (4.93 g, 18.20 mmol), sodium carbonate (10.52 g, 99 mmol), and tetrakis-(triphenylphosphine)palladium(0) (1.338 g, 1.158 mmol) were combined in a flask, and 400 mL of 1,2-dimethoxyethane was added with ethanol (26.7 mL) and water (33.3 mL). The reaction mixture was heated with stirring at 80 °C for 30 h. The reaction progress was monitored by LC-MS. Upon completion of the reaction, the mixture was cooled to room temperature and the product precipitated. Solids were collected by filtration, washed with cold water, and air-dried, affording **18** (5.35 g, 14.40 mmol, 87% yield). ^{1}H NMR (500 MHz, DMSO-d_6) δ: 12.40 (br s, 1H), 8.44 (d, J = 2.44 Hz, 1H), 8.22 (dd, J = 2.20, 8.55 Hz, 1H), 8.16 (d, J = 3.42 Hz, 1H), 8.07 (d, J = 8.30 Hz, 2H), 7.84 (d, J = 8.30 Hz, 2H), 7.80 (d, J = 8.79 Hz, 1H), 3.64 (t, J = 4.65 Hz, 4H), 2.91 (t, J = 4.65 Hz, 4H). MS: m/z = 372.2 $(M + H)^+$.

4-((4-(4-Chloroquinazolin-6-yl)phenyl)sulfonyl)morpholine Hydrochloride (19). Thionyl chloride (9.83 mL, 135 mmol) was added slowly to 1.0 g of **18** (1 g, 2.69 mmol), followed by *N*,*N*-

dx.doi.org/10.1021/jm400349k | J. Med. Chem. XXXX, XXX, XXX−XXX

dimethylformamide (2.085 μL, 0.027 mmol). The reaction mixture was refluxed for 36 h, monitoring reaction progress with LC-MS. The volatile components were removed via distillation, providing **19** (1.12 g, 1.683 mmol, 80% pure, 78% yield), which was used for subsequent reactions without further purification. ^{1}H NMR (500 MHz, DMSO-d_6) δ: 8.45 (d, J = 1.95 Hz, 1H), 8.32 (s, 1H), 8.26 (dd, J = 2.20, 8.55 Hz, 1H), 8.07 (d, J = 8.79 Hz, 2H), 7.79−7.86 (m, 3H), 3.65 (t, J = 4.60 Hz, 4H), 2.92 (t, J = 4.65 Hz, 4H). MS: m/z = 390.04 $(M + H)^+$.

6-(4-(Morpholinosulfonyl)phenyl)-*N*-arylquinazolin-4-amines hydrochloride **20** were synthesized following general procedure C. To a solution of **19** (100 μmol) in *N*,*N*-dimethylformamide (0.5 mL) was added aryl amine (110 μmol), and the mixture was heated on a shaker plate at 80 °C for 12 h. After cooling the reaction mixture to room temperature, 0.5 mL of 2-propanol was added. The resulting yellowish precipitate was filtered and washed with 2 mL of 2-propanol, affording the amines **20.**

6-(4-(Morpholinosulfonyl)phenyl)-*N*-phenylquinazolin-4-amine Hydrochloride (20a). Yield: 50.8%. ^{1}H NMR (500 MHz, DMSO-d_6) δ: 11.51 (br s, 1H), 9.20 (s, 1H), 8.93 (s, 1H), 8.50 (d, J = 8.79 Hz, 1H), 8.21 (d, J = 8.30 Hz, 2H), 8.01 (d, J = 8.30 Hz, 1H), 7.95 (d, J = 8.30 Hz, 2H), 7.75 (d, J = 8.30 Hz, 2H), 7.51−7.55 (m, 2H), 7.34−7.37 (m, 1H), 3.65−3.67 (br m, 4H), 2.92−2.95 (br m, 4H). MS: m/z = 447.2 $(M + H)^+$.

6-(4-(Morpholinosulfonyl)phenyl)-*N*-(*p*-tolyl)quinazolin-4-amine Hydrochloride (20b). Yield: 54.9%. ^{1}H NMR (500 MHz, DMSO-d_6) δ: 11.62 (br s, 1H), 9.24 (s, 1H), 8.93 (s, 1H), 8.51 (d, J = 8.30 Hz, 1H), 8.22 (d, J = 8.30 Hz, 3H), 8.03 (d, J = 8.79 Hz, 1H), 7.95 (d, J = 8.79 Hz, 2H), 7.63 (d, J = 7.81 Hz, 2H), 7.34 (d, J = 7.81 Hz, 2H), 3.67 (t, J = 4.4 Hz, 4H), 2.95 (t, J = 4.4 Hz, 4H), 2.38 (s, 3H). MS: m/z = 461.2 $(M + H)^+$.

2-Chloro-4-((6-(4-(morpholinosulfonyl)phenyl)quinazolin-4-yl)amino)phenol Hydrochloride (20c). Yield: 52.7%. ^{1}H NMR (500 MHz, DMSO-d_6) δ: 11.60 (br s, 1H), 10.55 (br s, 1H), 9.22 (s, 1H), 8.96 (s, 1H), 8.51 (dd, J = 1.47, 8.79 Hz, 1H), 8.22 (d, J = 8.30 Hz, 2H), 8.02 (d, J = 8.79 Hz, 1H), 7.95 (d, J = 8.30 Hz, 2H), 7.81 (d, J = 2.93 Hz, 1H), 7.52 (dd, J = 2.44, 8.79 Hz, 1H), 7.12 (d, J = 8.79 Hz, 1H), 3.7 (t, J = 4.40 Hz, 4H), 2.95 (t, J = 4.4 Hz, 4H). MS: m/z = 497.2 $(M + H)^+$.

***N*-(3-Chloro-4-methoxyphenyl)-6-(4-(morpholinosulfonyl)-phenyl)quinazolin-4-amine Hydrochloride (20d).** Yield: 43.4%. ^{1}H NMR (500 MHz, DMSO-d_6) δ: 11.34 (br s, 1H), 9.14 (s, 1H), 8.94 (s, 1H), 8.49 (d, J = 8.79 Hz, 1H), 8.20 (d, J = 8.79 Hz, 2H), 8.00 (d, J = 8.79 Hz, 1H), 7.96 (d, J = 8.30 Hz, 2H), 7.93 (d, J = 2.44 Hz, 1H), 7.70 (dd, J = 2.44, 8.79 Hz, 1H), 7.31 (d, J = 9.28 Hz, 1H), 3.93 (s, 3H), 3.67 (t, J = 4.6 Hz, 4H), 2.95 (t, J = 4.6 Hz, 4H). MS: m/z = 511.1 $(M + H)^+$.

***N*-(4-(Benzyloxy)-3-chlorophenyl)-6-(4-(morpholinosulfonyl)phenyl)quinazolin-4-amine Hydrochloride (20e).** Yield: 70.1%. ^{1}H NMR (500 MHz, DMSO-d_6) δ: 11.49 (br s, 1H), 9.18 (s, 1H), 8.95 (s, 1H), 8.50 (dd, J = 1.71, 8.55 Hz, 1H), 8.20−8.22 (m, 2H), 8.01 (d, J = 8.79 Hz, 1H), 7.93−7.96 (m, 3H), 7.68 (dd, J = 2.69, 9.03 Hz, 1H), 7.51−7.53 (m, 2H), 7.35−7.46 (m, 4H), 5.30 (s, 2H), 3.66−3.68 (t, J = 4.9 Hz, 4H), 2.5 (t, J = 4.4 Hz, 4H). MS: m/z = 587.2 $(M + H)^+$.

***N*-(4-((3-Bromobenzyl)oxy)-3-chlorophenyl)-6-(4-(morpholinosulfonyl)phenyl)quinazolin-4-amine Hydrochloride (20f).** Yield: 51.6%. ^{1}H NMR (500 MHz, DMSO-d_6) δ: 11.45 (br s, 1H), 9.17 (s, 1H), 8.95 (s, 1H), 8.50 (d, J = 8.79 Hz, 1H), 8.21 (d, J = 8.79 Hz, 2H), 8.01 (d, J = 8.30 Hz, 1H), 7.94−7.97 (m, 3H), 7.72 (s, 1H), 7.69 (dd, J = 2.69, 9.03 Hz, 1H), 7.58 (d, J = 7.81 Hz, 1H), 7.52 (d, J = 7.81 Hz, 1H), 7.37−7.43 (m, 2H), 5.31 (s, 2H), 3.67 (t, J = 4.4 Hz, 4H), 2.95 (t, J = 4.35 Hz, 4H). MS: m/z = 665.1 $(M + H)^+$.

***N*-(3-Chloro-4-((3-chlorobenzyl)oxy)phenyl)-6-(4-(morpholinosulfonyl)phenyl)quinazolin-4-amine Hydrochloride (20g).** Yield: 49.1%. ^{1}H NMR (500 MHz, DMSO-d_6) δ: 11.54 (br s, 1H), 9.19 (br s, 1H), 8.96 (br s, 1H), 8.50 (d, J = 8.79 Hz, 1H), 8.21 (d, J = 8.30 Hz, 2H), 7.98−8.08 (m, 1H), 7.94−7.96 (m, 3H), 7.69 (dd, J = 2.44, 8.79 Hz, 1H), 7.58 (br s, 1H), 7.37−7.50 (m, 4H), 5.31 (br s, 2H), 3.67 (br s, 4H), 2.95 (br s, 4H). MS: m/z = 621.1 $(M + H)^+$.

***N*-(3-Chloro-4-((2,3-difluorobenzyl)oxy)phenyl)-6-(4-(morpholinosulfonyl)phenyl)quinazolin-4-amine Hydrochloride (20h).** Yield: 53.3%. ^{1}H NMR (500 MHz, DMSO-d_6) δ: 11.58 (br s, 1H), 9.22 (s, 1H), 8.97 (s, 1H), 8.51 (dd, J = 1.46, 8.79 Hz, 1H), 8.22 (d, J = 8.30 Hz, 2H), 8.03 (d, J = 8.79 Hz, 1H), 7.93−7.97 (m, 3H), 7.73 (dd, J = 2.44, 8.79 Hz, 1H), 7.43−7.53 (m, 3H), 7.28−7.34 (m, 1H), 5.38 (s, 2H), 3.67 (t, J = 4.4 Hz, 4H), 2.95 (t, J = 4.6 Hz, 4H). MS: m/z = 623.2 $(M + H)^+$.

***N*-(3-Chloro-4-((2-fluorobenzyl)oxy)phenyl)-6-(4-(morpholinosulfonyl)phenyl)quinazolin-4-amine Hydrochloride (20i).** Yield: 41.2%. ^{1}H NMR (500 MHz, DMSO-d_6) δ: 11.32 (br s, 1H), 9.12 (br s, 1H), 8.93 (br s, 1H), 8.47 (d, J = 8.79 Hz, 1H), 8.18 (d, J = 8.30 Hz, 2H), 7.98 (d, J = 8.79 Hz, 1H), 7.92−7.96 (m, 3H), 7.70 (dd, J = 2.44, 8.79 Hz, 1H), 7.60−7.63 (m, 1H), 7.43−7.46 (m, 2H), 7.25−7.32 (m, 2H), 5.31 (s, 2H), 3.65 (t, J = 4.6 Hz, 4H), 2.93 (t, J = 4.6 Hz, 4H). MS: m/z = 605.2 $(M + H)^+$.

***N*-(3-Chloro-4-((4-fluorobenzyl)oxy)phenyl)-6-(4-(morpholinosulfonyl)phenyl)quinazolin-4-amine Hydrochloride (20j).** Yield: 67.1%. ^{1}H NMR (500 MHz, DMSO-d_6) δ: 11.66 (br s, 1H), 9.24 (br s, 1H), 8.97 (s, 1H), 8.52 (d, J = 8.79 Hz, 1H), 8.23 (d, J = 8.30 Hz, 2H), 8.03 (d, J = 8.79 Hz, 1H), 7.94−7.96 (m, 3H), 7.70 (dd, J = 2.44, 8.79 Hz, 1H), 7.55−7.58 (m, 2H), 7.41 (d, J = 8.79 Hz, 1H), 7.26−7.30 (m, 2H), 5.28 (s, 2H), 3.7 (t, J = 4.9 Hz, 4H), 2.95 (t, J = 4.6 Hz, 4H). MS: m/z = 605.2 $(M + H)^+$.

***N*-(3-Chloro-4-((3-methoxybenzyl)oxy)phenyl)-6-(4-(morpholinosulfonyl)phenyl)quinazolin-4-amine Hydrochloride (20k).** Yield: 43.1%. ^{1}H NMR (500 MHz, DMSO-d_6) δ: 11.40 (br s, 1H), 9.15 (s, 1H), 8.94 (s, 1H), 8.49 (d, J = 8.30 Hz, 1H), 8.20 (d, J = 8.30 Hz, 2H), 8.00 (d, J = 8.79 Hz, 1H), 7.93−7.97 (m, 3H), 7.68 (dd, J = 2.44, 8.79 Hz, 1H), 7.33−7.39 (m, 2H), 7.06−7.08 (m, 2H), 6.91−6.96 (m, 1H), 5.27 (s, 2H), 3.78 (s, 3H), 3.67 (t, J = 4.9 Hz, 4H), 2.95 (t, J = 4.4 Hz, 4H). MS: m/z = 617.2 $(M + H)^+$.

***N*-(3-Chloro-4-((3-fluoro-4-(trifluoromethyl)benzyl)oxy)-phenyl)-6-(4-(morpholinosulfonyl)phenyl)quinazolin-4-amine Hydrochloride (20l).** Yield: 40.9%. ^{1}H NMR (500 MHz, DMSO-d_6) δ: 11.74 (br s, 1H), 9.29 (s, 1H), 8.98 (s, 1H), 8.52 (dd, J = 1.46, 8.79 Hz, 1H), 8.24 (d, J = 8.79 Hz, 2H), 8.05 (d, J = 8.79 Hz, 1H), 7.99 (d, J = 2.44 Hz, 1H), 7.95 (d, J = 8.30 Hz, 2H), 7.89 (t, J = 7.81 Hz, 1H), 7.72 (dd, J = 2.44, 8.79 Hz, 1H), 7.63 (d, J = 11.23 Hz, 1H), 7.55 (d, J = 7.81 Hz, 1H), 7.38 (d, J = 8.79 Hz, 1H), 5.43 (s, 2H), 3.67 (t, J = 4.4 Hz, 4H), 2.95 (t, J = 4.4 Hz, 4H). MS: m/z = 673.2 $(M + H)^+$.

***N*-(3-Chloro-4-((2,3,5-trifluorobenzyl)oxy)phenyl)-6-(4-(morpholinosulfonyl)phenyl)quinazolin-4-amine Hydrochloride (20m).** Yield: 42%. ^{1}H NMR (500 MHz, DMSO-d_6) δ: 11.49 (br s, 1H), 9.19 (s, 1H), 8.96 (s, 1H), 8.51 (d, J = 9.77 Hz, 1H), 8.21 (d, J = 8.30 Hz, 2H), 8.02 (d, J = 8.79 Hz, 1H), 7.95−7.98 (m, 3H), 7.73 (dd, J = 2.69, 9.03 Hz, 1H), 7.56- 7.65 (m, 1H), 7.48 (d, J = 8.79 Hz, 1H), 7.34−7.36 (m, 1H), 5.38 (s, 2H), 3.67 (t, J = 4.9 Hz, 4H), 2.95 (t, J = 4.4 Hz, 4H). MS: m/z = 641.1 $(M + H)^+$.

***N*-(4-((3-Fluorobenzyl)oxy)phenyl)-6-(4-(morpholinosulfonyl)phenyl)quinazolin-4-amine (20n).** Yield: 45.8%. ^{1}H NMR (500 MHz, DMSO-d_6) δ: 11.40 (br s, 1H), 9.15 (s, 1H), 8.88 (s, 1H), 8.49 (d, J = 8.79 Hz, 1H), 8.20 (d, J = 8.79 Hz, 2H), 7.92−8.02 (m, 3H), 7.65 (d, J = 9.30 Hz, 2H), 7.45−7.51 (m, 1H), 7.31−7.35 (m, 2H), 7.16−7.22 (m, 3H), 5.21 (s, 2H), 3.67 (t, J = 4.4 Hz, 4H), 2.95 (t, J = 4.4 Hz, 4H). MS: m/z = 571.2 $(M + H)^+$.

***N*-(4-((3-Fluorobenzyl)oxy)-3-methoxyphenyl)-6-(4-(morpholinosulfonyl)phenyl)quinazolin-4-amine (20o).** Yield: 18%. ^{1}H NMR (500 MHz, DMSO-d_6) δ: 11.32 (br s, 1H), 9.14 (s, 1H), 8.90 (s, 1H), 8.49 (d, J = 8.30 Hz, 1H), 8.20 (d, J = 8.79 Hz, 2H), 7.99 (d, J = 8.79 Hz, 1H), 7.96 (d, J = 8.30 Hz, 2H), 7.45−7.50 (m, 1H), 7.41 (d, J = 2.44 Hz, 1H), 7.28−7.34 (m, 3H), 7.15−7.22 (m, 2H), 5.19 (s, 2H), 3.84 (s, 3H), 3.67 (t, J = 4.9 Hz, 4H), 2.95 (t, J = 4.4 Hz, 4H). MS: m/z = 601.1 $(M + H)^+$.

Trypanosome Replication Assays. Bloodstream *T. brucei brucei* Lister 427 cells were seeded at a density of 2 × 10^3 cells/mL and cultured in HMI-9 medium[47] in a 24-well plate. Then 2 μL of DMSO (control) or different concentrations of drugs prepared from 200× DMSO stocks were added to the cultures. Cells were incubated at 37 °C for 48 h and counted with a hemocytometer. Drugs were initially tested at concentrations of 10 μM, 1 μM, 100 nM, and 10 nM to

dx.doi.org/10.1021/jm400349k | J. Med. Chem. XXXX, XXX, XXX−XXX

determine the range of potency of each compound. Thereafter, a set of five concentrations centered around a dose that prevented replication of 50% of cells (compared to DMSO) was used to establish the EC_{50}. All experiments were repeated thrice in independent studies where each dose was administered in duplicate (total $n = 6$).

HepG2 Cell Toxicity Assay. The 384 well MTT cytotoxicity assay is a modification of the MTT method described by Ferrari et al.[48] optimized for 384-well throughput, with modifications described in detail in the Supporting Information. The 50% inhibitory concentrations (IC_{50}) were generated for each toxicity dose response test using GraphPad Prism (GraphPad Software Inc., San Diego, CA) using the nonlinear regression (sigmoidal dose–response/variable slope) equation.

■ ASSOCIATED CONTENT

Supporting Information

Synthesis of selected boronates and a tabulation of all the inhibitors, with their Northeastern registry numbers and screening data. Also included are biological assay details, data from pharmacokinetic, and in vivo efficacy studies, plasma protein binding, and results from cell cycle analysis following inhibitor treatment. This material is available free of charge via the Internet at http://pubs.acs.org.

■ AUTHOR INFORMATION

Corresponding Author

*For M.P.P., medicinal chemistry: phone, 617-373-2703; E-mail, m.pollastri@neu.edu. For K.M.-W., biology: 706-542-3355; E-mail, mensawil@uga.edu.

Author Contributions

M.P.P. developed the medicinal chemistry strategy and contributed to compound designs. K.M.-W. initiated the project. G.P., C.E.K., and P.E. contributed to compound designs and performed chemical synthesis and characterization. R.B., P.G., and C.S. performed trypanosome assays, and N.E.R. performed the HepG2 assays.

Notes

The authors declare no competing financial interest.

■ ACKNOWLEDGMENTS

Funding from the National Institutes of Health (R01AI082577 to M.P., and R21AI076647 to K.M.-W.), the National Science Foundation (MCB-0843603), Northeastern University, and a gift of compounds (Table 1) from GlaxoSmithKline, Inc.. is gratefully acknowledged. We appreciate helpful discussions with Dr. Richard Sciotti at Walter Reed Army Institute of Research and Dr. Franco Lombardo at Novartis.

■ ABBREVIATIONS USED

EGFR, epidermal growth factor receptor; EC_{50}, concentration at which cell growth is inhibited by 50%; FDA, Food and Drug Administration; MTT, 3-(4,5-dimethylthiazol-2-yl)-2,5-diphenyltetrazolium bromide; PDE, phosphodiesterase

■ REFERENCES

(1) *Uniting to Combat NTDs Homepage*; www.unitingtocombatntds.org, 2013; (accessed 12 April 2013).

(2) Pollastri, M. P.; Campbell, R. K. Target repurposing for neglected diseases. *Future Med. Chem.* **2011**, *3*, 1307–1315.

(3) Gould, M. K.; de Koning, H. P. Cyclic-nucleotide signalling in protozoa. *FEMS Microbiol. Rev.* **2011**, *35*, 515–541.

(4) Parsons, M.; Worthey, E. A.; Ward, P. N.; Mottram, J. C. Comparative analysis of the kinomes of three pathogenic trypanosomatids: *Leishmania major*, *Trypanosoma brucei* and *Trypanosoma cruzi*. *BMC Genomics* **2005**, *6*, 127.

(5) Bland, N. D.; Wang, C.; Tallman, C.; Gustafson, A. E.; Wang, Z.; Ashton, T. D.; Ochiana, S. O.; McAllister, G.; Cotter, K.; Fang, A. P.; Gechijian, L.; Garceau, N.; Gangurde, R.; Ortenberg, R.; Ondrechen, M. J.; Campbell, R. K.; Pollastri, M. P. Pharmacological validation of *Trypanosoma brucei* phosphodiesterases B1 and B2 as druggable targets for African sleeping sickness. *J. Med. Chem.* **2011**, *54*, 8188–8194.

(6) Ochiana, S. O.; Pandarinath, V.; Wang, Z.; Kapoor, R.; Ondrechen, M. J.; Ruben, L.; Pollastri, M. P. The human Aurora kinase inhibitor danusertib is a lead compound for anti-trypanosomal drug discovery via target repurposing. *Eur. J. Med. Chem.* **2012**, *62*, 777–784.

(7) Diaz-Gonzalez, R.; Kuhlmann, F. M.; Galan-Rodriguez, C.; Madeira da Silva, L.; Saldivia, M.; Karver, C. E.; Rodriguez, A.; Beverley, S. M.; Navarro, M.; Pollastri, M. P. The susceptibility of trypanosomatid pathogens to PI3/mTOR kinase inhibitors affords a new opportunity for drug repurposing. *PLoS Negl. Trop. Dis.* **2011**, *5*, e1297.

(8) de Koning, H. P.; Gould, M. K.; Sterk, G. J.; Tenor, H.; Kunz, S.; Luginbuehl, E.; Seebeck, T. Pharmacological validation of *Trypanosoma brucei* phosphodiesterases as novel drug targets. *J. Infect. Dis.* **2012**, *206*, 229–237.

(9) Beghyn, T. B.; Charton, J.; Leroux, F.; Laconde, G.; Bourin, A.; Cos, P.; Maes, L.; Deprez, B. Drug to genome to drug: discovery of new antiplasmodial compounds. *J. Med. Chem.* **2011**, *54*, 3222–3240.

(10) Nwaka, S.; Hudson, A. Innovative lead discovery strategies for tropical diseases. *Nature Rev. Drug Discovery* **2006**, *5*, 941–955.

(11) Chahrour, O.; Cairns, D.; Omran, Z. Small molecule kinase inhibitors as anti-cancer therapeutics. *Mini-Rev. Med. Chem.* **2012**, *12*, 399–411.

(12) Page, T. H.; Smolinska, M.; Gillespie, J.; Urbaniak, A. M.; Foxwell, B. M. Tyrosine kinases and inflammatory signalling. *Curr. Mol. Med.* **2009**, *9*, 69–85.

(13) Ito, K.; Caramori, G.; Adcock, I. M. Therapeutic Potential of Phosphatidylinositol 3-Kinase Inhibitors in Inflammatory Respiratory Disease. *J. Pharmacol. Exp. Ther.* **2007**, *321*, 1–8.

(14) Louvet, C.; Szot, G. L.; Lang, J.; Lee, M. R.; Martinier, N.; Bollag, G.; Zhu, S.; Weiss, A.; Bluestone, J. A. Tyrosine kinase inhibitors reverse type 1 diabetes in nonobese diabetic mice. *Proc. Natl. Acad. Sci. U. S. A.* **2008**, *105*, 18895–18900.

(15) Wagman, A. S.; Johnson, K. W.; Bussiere, D. E. Discovery and development of GSK3 inhibitors for the treatment of type 2 diabetes. *Curr. Pharm. Des.* **2004**, *10*, 1105–1137.

(16) Chico, L. K.; Van Eldik, L. J.; Watterson, D. M. Targeting protein kinases in central nervous system disorders. *Nature Rev. Drug Discovery* **2009**, *8*, 892–909.

(17) Natoli, C. Tyrosine Kinase Inhibitors. *Curr. Cancer Drug Targets* **2010**, *10*, 462.

(18) Lackey, K. E. Lessons from the drug discovery of lapatinib, a dual ErbB1/2 tyrosine kinase inhibitor. *Curr. Top. Med. Chem.* **2006**, *6*, 435–460.

(19) Johannessen, L. E.; Ringerike, T.; Molnes, J.; Madshus, I. H. Epidermal growth factor receptor efficiently activates mitogen-activated protein kinase in HeLa cells and Hep2 cells conditionally defective in clathrin-dependent endocytosis. *Exp. Cell Res.* **2000**, *260*, 136–145.

(20) Naula, C.; Parsons, M.; Mottram, J. C. Protein kinases as drug targets in trypanosomes and *Leishmania*. *Biochim. Biophys. Acta* **2005**, *1754*, 151–159.

(21) Oduor, R. O.; Ojo, K. K.; Williams, G. P.; Bertelli, F.; Mills, J.; Maes, L.; Pryde, D. C.; Parkinson, T.; Van Voorhis, W. C.; Holler, T. P. *Trypanosoma brucei* Glycogen Synthase Kinase-3, A Target for Anti-Trypanosomal Drug Development: A Public–Private Partnership to Identify Novel Leads. *PLoS Negl. Trop. Dis.* **2011**, *5*, e1017.

(22) Nett, I. R.; Martin, D. M.; Miranda-Saavedra, D.; Lamont, D.; Barber, J. D.; Mehlert, A.; Ferguson, M. A. The phosphoproteome of bloodstream form *Trypanonosoma brucei*, causative agent of African sleeping sickness. *Mol. Cell Proteomics* **2009**, *8*, 1527–1538.

(23) Nett, I. R.; Davidson, L.; Lamont, D.; Ferguson, M. A. Identification and specific localization of tyrosine-phosphorylated proteins in *Trypanosoma brucei*. *Eukaryotic Cell* **2009**, *8*, 617−626.
(24) Katiyar, S.; Kufareva, I.; Behera, R.; Ogata, Y.; Pollastri, M. P.; Abagyan, R.; Mensa-Wilmot, K. Lapatinib-Binding Protein Kinases in the African Trypanosome: A General Method for Identification of Targets for Kinase-Directed Drugs in a Cell. *PLoS One* **2013**, *8*, e56150.
(25) Slichenmyer, W. J.; Elliott, W. L.; Fry, D. W. CI-1033, a pan-erbB tyrosine kinase inhibitor. *Semin. Oncol.* **2001**, *28*, 80−85.
(26) Xia, W.; Mullin, R. J.; Keith, B. R.; Liu, L. H.; Ma, H.; Rusnak, D. W.; Owens, G.; Alligood, K. J.; Spector, N. L. Anti-tumor activity of GW572016: a dual tyrosine kinase inhibitor blocks EGF activation of EGFR/erbB2 and downstream Erk1/2 and AKT pathways. *Oncogene* **2002**, *21*, 6255−6263.
(27) Traxler, P.; Allegrini, P. R.; Brandt, R.; Brueggen, J.; Cozens, R.; Fabbro, D.; Grosios, K.; Lane, H. A.; McSheehy, P.; Mestan, J.; Meyer, T.; Tang, C.; Wartmann, M.; Wood, J.; Caravatti, G. AEE788: a dual family epidermal growth factor receptor/ErbB2 and vascular endothelial growth factor receptor tyrosine kinase inhibitor with antitumor and antiangiogenic activity. *Cancer Res.* **2004**, *64*, 4931−4941.
(28) Steverding, D. The transferrin receptor of *Trypanosoma brucei*. *Parasitol. Int.* **2000**, *48*, 191−198.
(29) Subramanya, S.; Hardin, C. F.; Steverding, D.; Mensa-Wilmot, K. Glycosylphosphatidylinositol-specific phospholipase C regulates transferrin endocytosis in the African trypanosome. *Biochem. J.* **2009**, *417*, 685−694.
(30) Subramanya, S.; Mensa-Wilmot, K. Diacylglycerol-stimulated endocytosis of transferrin in trypanosomatids is dependent on tyrosine kinase activity. *PLoS One* **2010**, *5*, e8538.
(31) Behera, R.; Guyett, P.; Thomas, S.; Katiyar, S.; Ogata, Y.; Mensa-Wilmot, K.,unpublished results
(32) Rusnak, D. W.; Lackey, K.; Affleck, K.; Wood, E. R.; Alligood, K. J.; Rhodes, N.; Keith, B. R.; Murray, D. M.; Knight, W. B.; Mullin, R. J.; Gilmer, T. M. The effects of the novel, reversible epidermal growth factor receptor/ErbB-2 tyrosine kinase inhibitor, GW2016, on the growth of human normal and tumor-derived cell lines in vitro and in vivo. *Mol. Cancer Ther.* **2001**, *1*, 85−94.
(33) Petrov, K. G.; Zhang, Y. M.; Carter, M.; Cockerill, G. S.; Dickerson, S.; Gauthier, C. A.; Guo, Y.; Mook, R. A., Jr.; Rusnak, D. W.; Walker, A. L.; Wood, E. R.; Lackey, K. E. Optimization and SAR for dual ErbB-1/ErbB-2 tyrosine kinase inhibition in the 6-furanylquinazoline series. *Bioorg. Med. Chem. Lett.* **2006**, *16*, 4686−4691.
(34) Rusnak, D. W.; Affleck, K.; Cockerill, S. G.; Stubberfield, C.; Harris, R.; Page, M.; Smith, K. J.; Guntrip, S. B.; Carter, M. C.; Shaw, R. J.; Jowett, A.; Stables, J.; Topley, P.; Wood, E. R.; Brignola, P. S.; Kadwell, S. H.; Reep, B. R.; Mullin, R. J.; Alligood, K. J.; Keith, B. R.; Crosby, R. M.; Murray, D. M.; Knight, W. B.; Gilmer, T. M.; Lackey, K. The characterization of novel, dual ErbB-2/EGFR, tyrosine kinase inhibitors: potential therapy for cancer. *Cancer Res.* **2001**, *61*, 7196−7203.
(35) Cai, X.; Zhai, H.-X.; Wang, J.; Forrester, J.; Qu, H.; Yin, L.; Lai, C.-J.; Bao, R.; Qian, C. Discovery of 7-(4-(3-Ethynylphenylamino)-7-methoxyquinazolin-6-yloxy)-*N*-hydroxyheptanamide (CUDC-101) as a Potent Multi-Acting HDAC, EGFR, and HER2 Inhibitor for the Treatment of Cancer. *J. Med. Chem.* **2010**, *53*, 2000−2009.
(36) Hopkins, A. L.; Groom, C. R.; Alex, A. Ligand efficiency: a useful metric for lead selection. *Drug Discovery Today* **2004**, *9*, 430−431.
(37) Webster, P.; Fish, W. R. Endocytosis by African trypanosomes. II. Occurrence in different life-cycle stages and intracellular sorting. *Eur. J. Cell Biol.* **1989**, *49*, 303−310.
(38) Hall, B.; Allen, C. L.; Goulding, D.; Field, M. C. Both of the Rab5 subfamily small GTPases of *Trypanosoma brucei* are essential and required for endocytosis. *Mol. Biochem. Parasitol.* **2004**, *138*, 67−77.
(39) Hammarton, T. C. Cell cycle regulation in *Trypanosoma brucei*. *Mol. Biochem. Parasitol.* **2007**, *153*, 1−8.
(40) Siegel, T. N.; Hekstra, D. R.; Cross, G. A. Analysis of the *Trypanosoma brucei* cell cycle by quantitative DAPI imaging. *Mol. Biochem. Parasitol.* **2008**, *160*, 171−174.
(41) Hammarton, T. C.; Monnerat, S.; Mottram, J. C. Cytokinesis in trypanosomatids. *Curr. Opin. Microbiol.* **2007**, *10*, 520−527.
(42) Mackey, Z. B.; Baca, A. M.; Mallari, J. P.; Apsel, B.; Shelat, A.; Hansell, E. J.; Chiang, P. K.; Wolff, B.; Guy, K. R.; Williams, J.; McKerrow, J. H. Discovery of trypanocidal compounds by whole cell HTS of *Trypanosoma brucei*. *Chem. Biol. Drug Des.* **2006**, *67*, 355−363.
(43) Wager, T. T.; Chandrasekaran, R. Y.; Hou, X.; Troutman, M. D.; Verhoest, P. R.; Villalobos, A.; Will, Y. Defining Desirable Central Nervous System Drug Space through the Alignment of Molecular Properties, in Vitro ADME, and Safety Attributes. *ACS Chem. Neurosci.* **2010**, *1*, 420−434.
(44) Wager, T. T.; Hou, X.; Verhoest, P. R.; Villalobos, A. Moving beyond Rules: The Development of a Central Nervous System Multiparameter Optimization (CNS MPO) Approach To Enable Alignment of Druglike Properties. *ACS Chem. Neurosci.* **2010**, *1*, 435−449.
(45) Iino, T.; Sasaki, Y.; Bamba, M.; Mitsuya, M.; Ohno, A.; Kamata, K.; Hosaka, H.; Maruki, H.; Futamura, M.; Yoshimoto, R.; Ohyama, S.; Sasaki, K.; Chiba, M.; Ohtake, N.; Nagata, Y.; Eiki, J.-i.; Nishimura, T. Discovery and structure−activity relationships of a novel class of quinazoline glucokinase activators. *Bioorg. Med. Chem. Lett.* **2009**, *19*, 5531−5538.
(46) Mahboobi, S.; Sellmer, A.; Winkler, M.; Eichhorn, E.; Pongratz, H.; Ciossek, T.; Baer, T.; Maier, T.; Beckers, T. Novel Chimeric Histone Deacetylase Inhibitors: A Series of Lapatinib Hybrids as Potent Inhibitors of Epidermal Growth Factor Receptor (EGFR), Human Epidermal Growth Factor Receptor 2 (HER2), and Histone Deacetylase Activity. *J. Med. Chem.* **2010**, *53*, 8546−8555.
(47) Hirumi, H.; Hirumi, K. Axenic culture of African trypanosome bloodstream forms. *Parasitol. Today.* **1994**, *10*, 80−84.
(48) Ferrari, M.; Fornasiero, M. C.; Isetta, A. M. MTT colorimetric assay for testing macrophage cytotoxic activity in vitro. *J. Immunol. Methods* **1990**, *131*, 165−172.
(49) Sykes, M. L.; Baell, J. B.; Kaiser, M.; Chatelain, E.; Moawad, S. R.; Ganame, D.; Ioset, J.-R.; Avery, V. M. Identification of Compounds with Anti-Proliferative Activity against *Trypanosoma brucei brucei* Strain 427 by a Whole Cell Viability Based HTS Campaign. *PLoS Negl. Trop. Dis.* **2012**, *6*, e1896.
(50) Sokolova, A. Y.; Wyllie, S.; Patterson, S.; Oza, S. L.; Read, K. D.; Fairlamb, A. H. Cross-resistance to nitro drugs and implications for treatment of human African trypanosomiasis. *Antimicrob. Agents Chemother.* **2010**, *54*, 2893−2900.
(51) Jacobs, R. T.; Nare, B.; Wring, S. A.; Orr, M. D.; Chen, D.; Sligar, J. M.; Jenks, M. X.; Noe, R. A.; Bowling, T. S.; Mercer, L. T.; Rewerts, C.; Gaukel, E.; Owens, J.; Parham, R.; Randolph, R.; Beaudet, B.; Bacchi, C. J.; Yarlett, N.; Plattner, J. J.; Freund, Y.; Ding, C.; Akama, T.; Zhang, Y. K.; Brun, R.; Kaiser, M.; Scandale, I.; Don, R. SCYX-7158, an Orally-Active Benzoxaborole for the Treatment of Stage 2 Human African Trypanosomiasis. *PLoS Negl. Trop. Dis.* **2011**, *5*, e1151.